Two separate roles for the transcription coactivator SAGA and a set of genes redundantly regulated by TFIID and SAGA

Rafal Donczew [1*], Linda Warfield[1*], Ariel Erijman[1,2] and Steven Hahn[1$]

* Equal contributions

[1]Fred Hutchinson Cancer Research Center,

1100 Fairview Ave N. A1-162, Seattle, WA 98109

[2] Present address: New England Biolabs, Ipswich, MA 01938

[$]Correspondence to Steven Hahn, shahn@fredhutch.org, 206 667 5261

Gene deletions in subunits of yeast coactivator SAGA reveal a general role in transcription linked to SAGA-regulated chromatin modifications. However, rapid SAGA depletion showed only a modest gene-specific role at 13% of expressed genes. These genes, termed "TFIID/SAGA-redundant genes", are generally more sensitive to rapid TFIID depletion than rapid SAGA depletion. Simultaneous depletion of both coactivators has a severe effect on transcription from this gene set, showing the overlapping role of both factors. The remaining 87% of expressed genes we term "TFIID-dependent" are highly sensitive to TFIID depletion and insensitive to rapid SAGA depletion. These two gene categories overlap, but have significant differences, with the previously defined "SAGA-dominated" and "TFIID-dominated" genes. Combined with earlier results, our findings suggest that the TFIID/SAGA-redundant genes can use either the TFIID or SAGA pathway for TBP-DNA loading. We also find that the gene-specific SAGA function is required for maintenance of transcription rather than activation.

Efficient in vitro transcription by RNA Pol II is initiated with six basal transcription factors (TATA binding protein (TBP), TFIIA, TFIIB, TFIIE, TFIIF, TFIIH), Pol II enzyme and TATA-containing promoter DNA. However, all cellular transcription, much of which initiates at non-TATA-containing promoters, additionally requires one or more coactivator complexes such as Mediator, TFIID, SAGA, NuA4 and Swi/Snf, that either directly contacts the basal transcription machinery and/or modifies chromatin (Allen and Taatjes, 2015; Doyon and Côté, 2004; Hahn and Young, 2011; Hantsche and Cramer, 2017; Nogales et al., 2017b; Rando and Winston, 2012; Sainsbury et al., 2015). Often recruited by transcription activators, coactivators play roles in processes such as promoter recognition, assembly of the basal factors into a functional preinitiation complex (PIC), catalysis of covalent chromatin modifications, nucleosome positioning, and stimulation of early steps in the transition from initiation to elongation. Although we know much about the structure, enzymatic functions, and protein-protein interactions for many of the above coactivators, relatively little is known about mechanisms that determine their genome-wide specificity and the molecular mechanisms of how they promote induction and maintenance of activated transcription.

31 The yeast coactivators SAGA and TFIID share 5 subunits (Grant et al., 1998) but are otherwise
32 unrelated. SAGA contains four known activities: activator binding, histone H3-acetylation,
33 histone H2B de ubiquitylation and relatively weak TBP binding (Han et al., 2014; Helmlinger et
34 al., 2011; K. K. Lee et al., 2011; Liu et al., 2019; Setiaputra et al., 2015). Because of its dual
35 functions in activator and TBP binding, it was proposed that SAGA assists TBP recruitment and
36 DNA binding, although details of this mechanism are unclear. TFIID is a large dynamic complex,
37 comprised of TBP and 13-14 Taf subunits, that functions in activator binding, promoter
38 recognition and PIC formation (Bieniossek et al., 2013; Hahn and Young, 2011; Nogales et al.,
39 2017a). Prior studies showed that TFIID can bind one or more short downstream metazoan
40 promoter elements and that it undergoes large conformational changes while positioning TBP
41 on DNA (Kolesnikova et al., 2018; Louder et al., 2016). CryoEM structures of human TFIID and
42 TFIIA-TFIID-DNA revealed that this complex seems incompatible with PIC formation (Patel et al.,
43 2018). Several Tafs in the DNA complex are in position to clash with TFIIF and Pol II in the PIC
44 and the DNA bend in the TFIIA-TFIID-DNA complex is different from that in the closed state PIC.
45 From this it was proposed that TFIID functions as a TBP-loading factor and that the Tafs must
46 either dissociate or undergo major rearrangement before PIC assembly. In this view, the final
47 state of TBP in functional PICs is the same, no matter which pathway was used for TBP
48 recruitment.
49
50 The genome-wide specificity of SAGA and TFIID have been the subject of much investigation.
51 Early work showed that at least some yeast genes can be activated and transcribed after
52 depletion or inactivation of TFIID Tafs (Kuras et al., 2000; Li et al., 2000; Moqtaderi et al., 1996;
53 Walker et al., 1996). Pioneering genome-wide studies later suggested that both TFIID and SAGA
54 contribute to steady state mRNA expression of most genes, but that expression at nearly all
55 yeast promoters is dominated by the dependence on either TFIID or SAGA (Huisinga and Pugh,
56 2004). From this study, the TFIID-dominated class represented ~ 90% of Pol II-transcribed
57 genes, many of which lacked a consensus TATA element, while the SAGA-dominated genes are
58 enriched for TATA-containing and stress-inducible genes. Formaldehyde crosslinking methods
59 showed that promoters from the TFIID-dominated class generally have high levels of TFIID-

60 subunit crosslinking while lower levels of crosslinking is often observed at the SAGA-dominated
61 genes (Kuras et al., 2000; Li et al., 2000; Rhee and Pugh, 2012).
62
63 Several subsequent findings challenged these initial models. First, mutations affecting genome-
64 wide transcription are now known to alter mRNA stability, making prior steady state mRNA
65 measurements used in earlier studies of TFIID and SAGA specificity problematic (Haimovich et
66 al., 2013; Munchel et al., 2011; Sun et al., 2012). Second, mapping SAGA-dependent chromatin
67 modifications showed that SAGA modifies chromatin at nearly all expressed genes, rather than
68 only at the SAGA-dominated subset (Bonnet et al., 2014). Third, formaldehyde-independent
69 mapping of SAGA and TFIID using the ChEC-seq approach identified TFIID and SAGA binding at
70 both gene classes (Baptista et al., 2017; Donczew et al., submitted.; Grünberg et al., 2016).
71 Finally, native Pol II ChIP and/or analysis of newly-synthesized mRNA found that the majority of
72 genes showed decreased transcription upon deletion or depletion of SAGA or TFIID subunits
73 (Baptista et al., 2017; Warfield et al., 2017). However, the proposal that TFIID is generally
74 required for transcription was recently disputed based on anchor-away depletion of the TFIID
75 subunit Taf1, with transcription assayed by Pol II ChIP (Petrenko et al., 2019). Analysis of the
76 top 10% of transcribed genes showed that many of these genes, enriched in the "SAGA-
77 dominated" class, were only modestly sensitive to Taf1 depletion.
78
79 Here we have investigated the discrepancies in TFIID and SAGA specificity raised by these prior
80 studies using 4-thioU RNA-seq to measure genome-wide transcription defects upon depletion
81 of SAGA and/or TFIID. This method, which measures newly synthesized RNA, has greater
82 sensitivity and lower background than approaches used in earlier studies and allows reliable
83 quantitation for ≥83% of yeast genes upon factor depletion. Using this approach, we find that
84 SAGA has two separable functions in gene expression: (1) a general function important for
85 transcription of nearly all genes that was revealed by deletions in genes encoding key SAGA
86 subunits and (2) a gene-specific role revealed by rapid depletion of SAGA function, where only
87 13% of genes are modestly affected. Surprisingly, this gene set is, on average, more sensitive to
88 rapid TFIID depletion. These and other results suggest that TFIID and SAGA function is

89 substantially redundant at this set of co-regulated genes, we term “TFIID/SAGA-redundant”
90 rather than “SAGA-dominated” or “Taf-independent” as previously proposed. The other 87% of
91 yeast genes, we term “TFIID-dependent” are very sensitive to rapid TFIID depletion but show
92 little or no change upon rapid SAGA depletion. Finally, at the coactivator-redundant genes, we
93 find that SAGA plays a significant role in maintenance of ongoing transcription rather than
94 activation per se.
95
96 **Results**
97 **SAGA has two separate roles in transcription**
98 To investigate the basis for conflicting reports on the genome-wide roles of SAGA and TFIID, we
99 used 4-thioU RNA-seq to quantitate transcriptional changes that are caused by various SAGA
100 depletion strategies. Yeast were grown in synthetic or rich glucose media and RNAs labeled for
101 5 min, followed by purification of the labeled RNA and quantitation by sequencing. This method
102 has much higher sensitivity and lower background compared with Pol II ChIP and allows
103 reproducible quantitation of newly-synthesized mRNA from ≥83% of Pol II-transcribed genes as
104 detailed in Materials and methods. Experiments, except where noted, were performed in
105 triplicate and there was low variation across the set of analyzed genes (**Fig S1A,B**).
106
107 We first examined genome-wide transcription changes caused by deletions in the SAGA
108 subunits: *spt3Δ*, *spt7Δ*, or *spt20Δ* or by rapid depletion of several SAGA subunits using the
109 auxin-degron system (Nishimura et al., 2009). The degron strains were designed to allow
110 simultaneous depletion of two SAGA subunits, either Spt3 + Spt7 or Spt3 + Spt20. Spt3 can bind
111 TBP while Spt7 and Spt20 are important for the integrity of SAGA (Han et al., 2014; K. K. Lee et
112 al., 2011; Liu et al., 2019; Sterner et al., 1999). The degron-depletion approach was also applied
113 to the individual TFIID subunits Taf1, Taf7 and Taf13 that are located in different TFIID lobes
114 (Patel et al., 2018; Warfield et al., 2017) . Protein degradation was induced by adding the auxin
115 3-IAA for 30 min, after which time, ≤10% of protein remained (**Fig S2A, B**). **Fig 1A** shows a
116 striking difference in genome-wide transcription defects when comparing rapid inactivation of
117 SAGA, a strain containing an *SPT3* deletion, or rapid inactivation of Taf13 (also **Table S1, S2**). For

118 example, the *spt3Δ* strain showed strong genome-wide transcription defects for nearly all
119 genes while degron-induced inactivation of Spt3 + Spt20 caused only modest defects at a small
120 subset of genes. The strong decrease in genome-wide transcription in *SPT* deletion strains is in
121 good agreement with prior results obtained using dynamic transcriptome analysis (DTA) and 4-
122 thioU-labeled RNA (Baptista et al., 2017). Rapid depletion of Taf13, a key TBP-interacting
123 subunit located in TFIID lobe A, caused strong genome-wide transcription defects at most genes
124 as previously observed using native Pol II ChIP (Warfield et al., 2017).
125
126 To determine whether subsets of genes are differentially affected by any of these depletion
127 strategies, the $\log_2$ change in transcription values from the SAGA deletion strains and TFIID-
128 degron strains were clustered by k-means algorithm with the results shown in **Fig 1B** and **Table**
129 **S3**. Grouping into two clusters showed two sets of genes that respond differently to TFIID or
130 SAGA depletion. The clustering was very robust as we obtained >95% overlap in gene categories
131 when we clustered using results from the SAGA-degron strains instead of the *SPT* deletion
132 strains. The largest cluster, we term "TFIID-dependent genes" (see reasoning below), contains
133 87% of analyzed genes (4245 genes) and is most sensitive to TFIID depletion. These genes show
134 a ~4.5-fold average decrease in transcription upon depletion of ether Taf13, Taf7 or Taf1 (**Fig**
135 **1B**, orange boxes, lanes 7-10). Results for the Taf13-degron are very similar when cells are
136 grown in either synthetic complete (SC) or rich (YPD) glucose media with excellent correlations
137 between Taf1, 7 and 13 depletions (**Fig S1C**). This large gene set was also sensitive to gene
138 deletions in SAGA subunits with genome-wide transcription decreased by an average of ~2.7-
139 fold in the *spt3Δ* strain with lesser but significant defects observed in the *spt7Δ* and *spt20Δ*
140 strains (**Fig 1B**, orange boxes, lanes 4-6). However, expression of nearly all genes in the "TFIID-
141 dependent" set showed little or no change upon rapid SAGA subunit depletion using the
142 Spt3+20 and Spt3+7 degron strains (**Fig 1B,** orange boxes, lanes 1-3).
143
144 The smaller gene set, that we term "TFIID/SAGA-redundant", contains 13% of analyzed genes
145 (655 genes) and these genes are more sensitive to deletions in SAGA subunits compared to
146 rapid TFIID depletion. Expression changes for these genes resulting from *SPT* deletions ranged

147 from ~3-4-fold (**Fig 1B**, blue boxes, lanes 4-6). In surprising contrast to the *SPT* deletion strains,
148 the TFIID/SAGA-redundant genes showed only modest transcription defects upon rapid SAGA
149 depletion (**Fig 1B**, blue boxes, lanes 1-3). The strongest average defect was caused by the
150 Spt3+Spt20 degron, with an average transcription change of ~1.6-fold. Combined, our results
151 show that there is a fundamental difference between cell growth for many generations in the
152 absence of SAGA vs rapid depletion of SAGA function. Surprisingly, quantitation of transcription
153 defects caused by rapid TFIID depletion vs rapid SAGA depletion showed that the TFIID/SAGA-
154 redundant genes are, on average, more sensitive to rapid depletion of TFIID (**Fig 1B**, blue boxes,
155 lanes 7-10). For example, we observed a ~2-fold average decrease in transcription in the Taf13-
156 degron vs ~1.6-fold decrease in the Spt3+20 degron.
157
158 The results above show that transcription of the TFIID/SAGA-redundant genes is not dominated
159 by either coactivator and suggests that TFIID and SAGA function is at least partially redundant
160 at this set of genes. To quantitate the extent of TFIID and SAGA redundancy at all genes, we
161 rapidly depleted both TFIID and SAGA using Taf13 + Spt3 and Taf13 + Spt7 double degron
162 strains. We found that simultaneous TFIID and SAGA depletion causes a severe defect in the
163 TFIID/SAGA-redundant genes with an average decrease of ~ 5.7-fold (**Fig 2A**, blue boxes, lanes
164 4-5); **Fig 2B** left panel, **Table S4**). For nearly all these genes, the transcription defect is greater
165 than simply the sum of the defects observed in the Taf13-degron and Spt3+20-degron (**Fig 2C**),
166 showing that there is substantial redundancy in the ability of TFIID and SAGA to promote
167 transcription of these genes. In contrast, the TFIID-dependent genes show, on average, no
168 additional defects in the double degron strains compared with the Taf13-degron (**Fig 2A**,
169 orange boxes, lanes 3-5); **Fig 2B** right panel, **Table S4**).
170
171 **Differences between "TFIID/SAGA-redundant" genes and "SAGA-dominated" genes**
172 Our "TFIID-dependent" and "TFIID/SAGA-redundant" gene sets overlap with the categories
173 previously defined: "TFIID-dominated" and "SAGA-dominated" (Huisinga and Pugh, 2004),
174 however, there are significant differences. Our TFIID/SAGA-redundant genes (655 genes)
175 contain 2/3 of the "SAGA-dominated" gene set (273 genes) plus an additional 311 genes that

176 were originally characterized as “TFIID-dominated” (**Fig S3A**). Therefore, our coactivator-
177 redundant gene set is over 50% different from the “SAGA-dominated” gene set. There are
178 corresponding differences in the “TFIID-dependent” vs “TFIID-dominated” gene set. We suspect
179 that these differences are mainly due to technical issues such as measurement of newly-
180 synthesized vs steady state mRNA and the greater sensitivity and depth of the 4-thioU RNA-seq
181 data compared with the microarray data used in the original analysis. These new results differ
182 from our prior Pol II ChIP experiments that did not detect gene-specific Taf requirements
183 (Warfield et al., 2017). However, it was recently suggested that this may be due to background
184 issues with Pol II ChIP data (e.g., stalled or paused Pols) and that Pol II ChIP is best used for
185 quantitation of changes in highly expressed genes (Petrenko et al., 2019). This explanation is
186 consistent with our new findings.
187
188 Importantly, our reclassification of many genes affects the interpretation of published studies
189 examining coactivator function and specificity that relied on the “SAGA-dominated” and “TFIID-
190 dominated” gene lists. For example, our prior collaborative study measured gene expression
191 defects upon rapid depletion of SAGA subunit Spt7 by anchor away (Baptista et al., 2017).
192 These results showed that expression of genes in both the “SAGA-dominated” and “TFIID-
193 dominated” gene categories are sensitive to rapid SAGA inactivation, in apparent contrast to
194 the SAGA-degron results reported here. However, comparing the specific genes tested in this
195 earlier work with our revised gene categories shows that 4/6 of the “TFIID-dominated” genes
196 assayed by Spt7 anchor away are in fact in the new TFIID/SAGA-redundant gene class and are
197 expected to be sensitive to rapid SAGA depletion. Therefore, the Spt7 anchor away results from
198 the earlier study are largely consistent with our current findings.
199
200 **Features of the TFIID-dependent and TFIID/SAGA-redundant gene classes**
201 When genes are sorted by transcription levels, determined by the amount of 4-thioU
202 incorporated in 5 min, the ratio of TFIID/SAGA to TFIID genes is relatively similar across most
203 genes, except for the most highly expressed (**Fig 3A, Fig S3B**). The bottom four expression
204 quintiles have a relatively constant ratio of ~10%, but the fraction of genes in the TFIID/SAGA

205 category increases to ~30% in the top quintile and ~44% in the top 10% of expressed genes. The
206 fraction of these genes increases even more dramatically when examining only the most highly
207 expressed genes. Yeast Pol II transcription is dominated by a small number of very highly
208 transcribed genes: the top 2% of expressed genes accounts for ~22% of total transcription (**Fig**
209 **3B; Fig S3C; Table S1**). As an example of the coactivator bias in the exceptionally highly
210 transcribed genes, of the top 50 expressed genes (expression >195 in Fig 3B), 47 (94%) are in
211 the coactivator-redundant category (**Table S3**).
212
213 Since genes in the TFIID/SAGA-redundant gene class are enriched in highly expressed genes, we
214 asked whether the sensitivity of individual genes in this set to rapid TFIID or SAGA depletion
215 varies with expression. For example, are highly expressed genes more sensitive to rapid SAGA
216 depletion vs TFIID depletion? **Fig 3C** shows a plot of the difference in sensitivity of genes to
217 rapid Taf13 and Spt3+7 depletion vs gene expression rank. From this plot, it is apparent that
218 most (68%) of the coactivator-redundant genes are more sensitive to Taf13-depletion
219 compared with rapid SAGA depletion (mean difference -0.49). This ratio changes slightly when
220 considering only the top 100 expressed genes where 49% show stronger TFIID vs SAGA-
221 dependence (mean difference -0.07). Combined, our analysis shows that the relative ratio of
222 TFIID vs SAGA-dependence of this gene set is not a barrier to very high levels of transcription.
223
224 It was previously noted that the "SAGA-dominated" genes are enriched for TATA-containing
225 promoters (Huisinga and Pugh, 2004), and the gene classes "SAGA-dominated" and "TATA-
226 containing" are often equated in the literature (TATA was defined as TATAWAWR; (Basehoar et
227 al., 2004)). To investigate this, we used the list of TATA-like elements defined in (Rhee and
228 Pugh, 2012) obtained from the YeasTSS database (www.yeastss.org), extracted the sequences
229 of all annotated TATA-elements and reclassified promoters as TATA-containing/TATA-less based
230 on the 7 nt consensus (TATAWAW). Although TATA-containing promoters are enriched, the
231 TFIID/SAGA-redundant class is clearly not equivalent to TATA-containing genes (**Fig 3D**) as there
232 are about equal numbers of genes from both classes that contain TATA and about equal
233 numbers of TFIID/SAGA-redundant genes that were classified as TATA or TATA-less.

234

235 The 136 ribosomal protein (RP) genes have sometimes been analyzed as a distinct category of
236 highly expressed and especially TFIID-dependent genes. From analysis of our new data, we did
237 not find that these genes are obviously distinct from many other genes based on TFIID or SAGA-
238 dependence. Although 95% of the RP genes belong to the TFIID-dependent category they show
239 comparable transcription defects as the rest of the TFIID-dependent genes. However, RP genes
240 are clearly more highly expressed than the average gene, with 83% of the RP genes in
241 expression quintile 5 (**Fig S4**). K-means clustering, based on TFIID and SAGA-dependence, with
242 up to 6 clusters, did not segregate the RP genes into a distinct category. Alternative methods
243 we applied (hierarchical and spectral clustering) also did not separate RP genes into a distinct
244 category. This analysis shows that RP genes have TFIID and SAGA-dependence similar to many
245 other genes. There can be good biological reasons to examine properties of RP genes as a
246 separate category since they are regulated coordinately in response to several signaling
247 pathways and this regulation is key for proper cellular growth and stress response. However,
248 they do not seem exceptional in regard to TFIID and SAGA-dependence.

249

250 **SAGA-regulated chromatin modifications change little during rapid SAGA inactivation**

251 We next investigated the basis for the difference in gene expression changes caused by the
252 SAGA deletion vs degron strains. SAGA was proposed to function through direct protein-protein
253 interactions to assist with TBP recruitment and PIC formation as well as through chromatin
254 changes mediated by Gcn5 and Ubp8 (Koutelou et al., 2010; Laprade et al., 2007; Mohibullah
255 and Hahn, 2008; Rodriguez-Navarro, 2009; Sermwittayawong and Tan, 2006). One possibility is
256 that transcription defects caused by rapid depletion are primarily mediated by disruption of key
257 protein-protein interactions, while the long-term effects of the *SPT* deletions are mediated in
258 part through changes in chromatin modifications.

259

260 To test this model, we measured SAGA-regulated chromatin changes (Daniel et al., 2004; Henry
261 et al., 2003; Morris et al., 2007) at times up to 2 hours after auxin addition to the Spt3+7 and
262 Spt3+20 degron strains. Western blot analyses of whole cell extracts showed that the *spt3Δ*,

263 *spt20Δ* and *spt7Δ* strains all had lower levels of the SAGA-regulated marks H3K18-acetyl and
264 H2B-Ub, ranging from 12-38% of normal (**Fig 4A**). Higher levels of H2B-Ub are observed upon
265 deletion of SAGA subunit Ubp8, the H2B deubiquitinase, but the lower levels of H2B-Ub
266 observed in the *SPT* deletion strains are unexpected. However, these strains all show lower
267 levels of genome-wide transcription and the deposition of the H2B-Ub mark is transcription-
268 dependent (Weake and Workman, 2008), providing a likely explanation for the lower levels.
269 Consistent with the suggestion that defects in SAGA-regulated chromatin modifications lead to
270 widespread transcription changes, it was reported that a strain with deletions in both *UPB8* and
271 *GCN5* has widespread defects in genome-wide transcription (Baptista et al., 2017). Importantly,
272 neither chromatin mark consistently changes more than ~10% after up to two hours post auxin
273 addition to the Spt3 + 20 and Spt3 + 7 double degron strains (**Fig 4B**). From these combined
274 results, we suggest that defects in SAGA-regulated chromatin modifications caused by the *SPT*
275 deletions are a major contributor to the genome-wide decrease in transcription observed at
276 nearly all genes. Since these chromatin modifications change little after 30 min of Auxin
277 treatment in the SAGA-degron strains, we propose that transcription changes caused by degron
278 depletion of SAGA (30 min) are most likely due to disrupting direct protein-protein interactions
279 between SAGA and other factors.
280
281 **Rapid SAGA depletion primarily affects maintenance of ongoing transcription rather than**
282 **gene activation by Gcn4**
283 Prior work showed that SAGA subunit deletion strains are defective in transcription activation
284 at some genes (Bhaumik and Green, 2001; Dudley et al., 1999; Mohibullah and Hahn, 2008). To
285 extend this work, we asked whether rapid SAGA depletion led to defects in activation of
286 transcription and/or in maintenance of activated and ongoing transcription. Strains were grown
287 in synthetic glucose media and RNA labeled for 5 min with 4-thioU followed by RT qPCR analysis
288 of newly-synthesized mRNA. Transcription was first measured in either the *spt3Δ* or *spt7Δ*
289 strains before or after addition of sulfometuron methyl (SM), which induces amino acid
290 starvation and induction of Gcn4-dependent genes (**Fig 5A; Fig S5**). Transcription was measured
291 at three TFIID-dependent genes (*ACT1, RPS5, SSH1*) that are not Gcn4 targets and three

292 TFIID/SAGA-redundant genes that are direct Gcn4 targets (*ARG3, HIS4, ARG5*). Compared with a
293 wild type strain, the SAGA deletion strains had lower expression levels at all three TFIID-
294 dependent genes and these genes showed little or no SM induction as expected. At the three
295 Gcn4 target genes, uninduced transcription was decreased compared with WT and the
296 response to SM was dependent on the *SPT* deletion. Although the levels of both uninduced and
297 activated transcription were reduced in the *spt7Δ* strain, the three Gcn4-dependent genes
298 showed some activation (light grey vs dark grey bars), while activation was eliminated in the
299 *spt3Δ* strain (light orange vs dark orange bars).
300
301 To determine the consequence of rapid SAGA depletion before transcription was induced, cells
302 containing the Spt3 + Spt7 double degrons were first treated with IAA for 30 min to deplete
303 these proteins and then induced with SM for 60 min. This treatment still allowed for normal
304 fold-activation upon subsequent SM addition (**Fig 5B** (light orange vs dark orange bars)). In
305 contrast, IAA added to already SM-induced cells reduced Gcn4-dependent transcription
306 between 1.7 and 2.6-fold (light vs dark grey bars). Combined, our results show that, for Gcn4-
307 dependent gene activation, SAGA is most important for maintenance of ongoing transcription
308 rather than necessary for gene activation per se.
309
310 **TFIID and SAGA map to both TFIID-dependent and coactivator-redundant genes**
311 As discussed above, there has been disagreement in prior work as to the location and amount
312 of TFIID binding to different gene classes. Formaldehyde-based crosslinking showed that Tafs
313 are generally depleted at the "SAGA-dominated" genes compared with the "TFIID-dominated
314 genes", while MNase-based ChEC showed similar binding to both gene classes. We revisited this
315 question using our revised gene lists, a modified ChEC-seq method, and higher stringency
316 criteria to map genome-wide binding of these two coactivators (Donczew et al., submitted.;
317 Tourigny et al., 2018). We found widespread promoter binding and ≥86% overlap in genes
318 bound by both these factors when comparing ChEC signals from Taf7 and Spt7-MNase fusions
319 (**Fig 6A**).
320

321 Further analysis of this data showed little or no preference for binding of these factors to either
322 promoter class (**Fig 6B**). Taf13, Taf7, Taf1, and Spt7 MNase fusions all gave similar ratios of
323 binding to each promoter type. The exception is the Spt3-MNase fusion that detected binding
324 at fewer TFIID-dependent promoters compared with the other MNase fusions. However, since
325 Spt3 is not known to be in any complex other than SAGA, we think it likely that this difference is
326 due to different DNA accessibility and/or the architecture of SAGA and other factors at the two
327 promoter types. Taken together, the widespread mapping of TFIID and SAGA at both promoter
328 types is consistent with SAGA and TFIID acting at nearly all genes.
329
330 **Discussion**
331 Here we have investigated the genome-wide and gene-specific roles for the coactivators SAGA
332 and TFIID. Several prior studies suggested that, while TFIID and SAGA make genome-wide
333 contributions, transcription at nearly all genes is dominated by one or the other factor and that
334 many highly-expressed genes show only modest TFIID-dependence (Huisinga and Pugh, 2004;
335 Petrenko et al., 2019). This view seemingly conflicts with other studies where TFIID and SAGA
336 were found to have major genome-wide roles at most genes (Baptista et al., 2017; Bonnet et
337 al., 2014; Warfield et al., 2017). Our new results bring together many of these findings and
338 provide a new mechanistic explanation for many of the genes that show significant Taf-
339 independent expression: TFIID and SAGA function is substantially redundant at these genes,
340 with WT expression levels promoted by both coactivators.
341
342 Rapid subunit depletion revealed two classes of genes with different dependencies on TFIID and
343 SAGA. The first class, termed TFIID-dependent genes, contains 87% of analyzed genes and
344 shows strong transcription dependence on TFIID but little or no change in response to rapid
345 depletion of SAGA. The second class, termed TFIID/SAGA-redundant genes (coactivator-
346 redundant), contains 13% of analyzed genes and shows modest transcription decreases in
347 response to rapid depletion of either TFIID or SAGA. Importantly, simultaneous depletion of
348 TFIID and SAGA leads to a severe transcription defect at the TFIID/SAGA genes. This latter result
349 is consistent with prior observations that the combination of SAGA and TFIID subunit mutations

350 results in greater transcription defects compared with either single mutation (Huisinga and
351 Pugh, 2004; T. I. Lee et al., 2000). Together, our results demonstrate that TFIID and SAGA have
352 partially redundant function at the TFIID/SAGA genes and, as described more fully below, we
353 envision that these genes can use either the TFIID or SAGA pathways to promote TBP binding
354 (**Fig 7**).
355
356 We also found that expression of nearly all genes is dependent on another function of SAGA
357 that is revealed in cells that have grown many generations without SAGA. Our results link this
358 genome-wide role to SAGA-regulated chromatin modifications - marks that are slow to change
359 upon rapid SAGA subunit depletion. Indirect effects, such as decreased expression of general
360 regulatory factors and components of the basal Pol II machinery, etc., likely also contribute to
361 lower genome-wide expression in the deletion strains. The two roles of SAGA seem additive,
362 which readily explains why the TFIID/SAGA-redundant genes are more sensitive to *SPT*
363 deletions compared to the TFIID-dependent genes. We propose that the coactivator-redundant
364 genes require both SAGA functions while the TFIID-dependent genes are primarily dependent
365 only on the SAGA-regulated chromatin modifications.
366
367 Yeast cellular transcription is dominated by a small number of exceptionally highly expressed
368 genes and it was proposed that highly expressed genes are biased for Taf-independent
369 expression (Petrenko et al., 2019). We do find that the TFIID/SAGA genes, while spread
370 throughout the range of expressed genes, are enriched in the top 10% of genes. However,
371 analysis of the ratio of SAGA-dependence/Taf-dependence shows that, within this entire gene
372 class, there is no obvious relationship between coactivator sensitivity and gene expression. In
373 fact, this analysis shows that most genes in the coactivator-redundant gene class show more
374 dependence on TFIID compared with SAGA.
375
376 Results from mapping the genome-wide locations of TFIID using a modified ChEC-seq method
377 are consistent with our findings that TFIID functions at both the TFIID-dependent and
378 TFIID/SAGA-redundant genes. We observe no bias in promoter type bound by TFIID or in the

379 ChEC-seq DNA cleavage patterns when comparing the two gene sets. Likewise, SAGA maps to
380 genes in both categories, consistent with its broad function at essentially all genes. In contrast,
381 prior studies have observed a bias in Taf-promoter binding using formaldehyde crosslinking. At
382 this time, the reason for this discrepancy is unknown, although we previously speculated that
383 the observed bias in proximity of TFIID to nucleosomes at TFIID-dependent genes (Rhee and
384 Pugh, 2012) may play a role in Taf-DNA crosslinking efficiency (Warfield et al., 2017).
385
386 From the above results, it is clear that the TFIID/SAGA-redundant genes are dependent on both
387 coactivators rather than expression being dominated by SAGA as proposed earlier; when one
388 coactivator is eliminated, the other can at least partially compensate. What is the mechanistic
389 basis for this behavior? Prior work suggests that both factors have overlapping functions in TBP
390 recruitment: TFIID clearly functions in TBP recruitment and SAGA has been proposed to have
391 this same function based on its TBP-binding and genetic interactions with TBP. Based on earlier
392 studies, we propose that the TFIID-dependent genes require Tafs for promoter recognition and
393 TBP-DNA loading. Most of these genes do not have a consensus TATA and therefore require
394 TFIID to properly position TBP at the site of PIC formation. We envision that the coactivator-
395 redundant genes can either load TBP using this same TFIID pathway or alternatively recruit TBP
396 more directly, taking advantage of: (1) specific TBP-TATA interactions and (2) direct TBP
397 interactions with other TBP-compatible DNA binding motifs. This model explains the surprising
398 viability of strains with TBP mutations that are defective in TATA-DNA binding (Kamenova et al.,
399 2014). These TBP mutants are predicted to be defective in the SAGA-mediated TBP loading
400 pathway but still function in the TFIID-dependent pathway. We note that these two gene
401 categories do not perfectly correlate with the presence or absence of TATA. It has been shown,
402 however, that the TATA consensus sequence does not perfectly correlate with function and
403 that sequences surrounding TATA are also important (Donczew and Hahn, 2018; Sprouse et al.,
404 2008)
405
406 The mechanistic role of SAGA in TBP recruitment and DNA loading is unclear as it has not been
407 demonstrated that SAGA directly assists TBP-DNA loading in an in vitro system. In any case,

408 based on the recent modeling of human TFIID-DNA and PICs (Patel et al., 2018), we propose
409 that the final state of the TBP-containing PIC is the same irrespective of the pathway used to
410 initiate TBP binding. In future studies, it will be very informative to isolate and compare
411 functional PICs formed using either pathway to test this prediction. Typically, only a small
412 fraction of PICs assembled in vitro are active, so this experiment has not yet been possible. A
413 transcription-dependent shift in Taf positioning has been recently observed and perhaps this
414 represents rearrangement of Tafs necessary for transcription initiation (Joo et al., 2017).
415
416 Finally, we found that rapid depletion of SAGA, primarily decreases ongoing and already
417 activated transcription at the TFIID/SAGA-redundant genes. In contrast, rapid depletion does
418 not affect activation per se at three Gcn4-dependent genes. This result is surprising, since it was
419 shown earlier that *SPT* deletion strains have defects in gene activation (Bhaumik and Green,
420 2001; Dudley et al., 1999). However, we now know that these strains are defective in both
421 functions of SAGA, unlike our rapid depletion experiments. Gene activation requires both a
422 permissive chromatin environment and efficient recruitment of TBP and other PIC components.
423 The activation process seems largely unaffected after rapid SAGA depletion, based on near-
424 normal ratios of induced/uninduced transcription of Gcn4-dependent genes. However, we did
425 find that rapid SAGA depletion reduced levels of ongoing and activated transcription at the
426 coactivator-redundant genes. Ongoing transcription, especially at highly expressed genes, likely
427 involves both transcription bursts and efficient transcription reinitiation. It is possible that SAGA
428 affects one or both of these processes and it will be of interest to probe for defects in these
429 steps in cells after rapid SAGA depletion.
430

431 **Materials and methods**

432 **Strain Construction**

433 *S. cerevisiae* and *S. pombe* strains were constructed using standard yeast methods. Proteins
434 were chromosomally tagged by high efficiency yeast transformation and homologous
435 recombination of PCR-amplified DNA. Plasmid pFA6a-3V5-IAA7-KanMX6 (Chan et al., 2018) was
436 used as the template for generating the IAA7 degron tags. This C-terminal tag contains three
437 copies of the V5 epitope tag followed by the IAA7 degron (32 kDa total).

438

439 **Yeast Cell Growth**

440 *S. cerevisiae* strains were grown in rich media (YPD) or synthetic media (glucose complete -Ile -
441 Val) as indicated and *S. pombe* strains were grown in YE media (0.5% yeast extract, 3% glucose).
442 *S. cerevisiae* strains at an A600 of ~ 1.0 were treated with 500 µM 3-IAA (or with DMSO) for 30
443 minutes, and with 0.5 µg/ml SM (or DMSO) for 60 minutes as described in the text and figure
444 legends, prior to RNA labeling.

445

446 **RNA Labeling and mRNA purification for RT-qPCR**

447 Newly synthesized RNAs were labeled as previously described (Bonnet et al., 2014). 10 ml *S.*
448 *cerevisiae* or 20 ml *S. pombe* cells were labeled with 5 mM 4-thiouracil (Sigma-Aldrich) for 5
449 minutes, the cells were pelleted at 3000 xg for 2 minutes, flash-frozen in liquid N_2, and then
450 stored at -80 deg C until further use. *S. cerevisiae* and *S. pombe* cells were mixed in an 8:1 ratio
451 and total RNA was extracted using the RiboPure yeast kit (Ambion, Life Technologies) using the
452 following volumes: 480 µl lysis buffer, 48 µl 10% SDS, 480 µl phenol:$CHCl_3$:IAA (25:24:1) per *S.*
453 *cerevisiae* pellet + 50 µl *S. pombe* (from a single *S. pombe* pellet resuspended in 850 µl lysis
454 buffer). Cells were lysed using 1.25 ml zirconia beads in a Mini Beadbeater-96 (BioSpec
455 Products) for 3 min followed by 1 min rest on ice. This bead beading cycle was repeated twice
456 for a total of 3 times. Lysates were spun for 5 min at 16K xg, then the following volumes
457 combined in a 5 ml tube: 400 µl supernatant, 1400 µl binding buffer, 940 µl 100% ethanol.
458 Samples were processed through the Ambion filter cartridges until all sample was loaded, then
459 washed with 700 µl Wash Solution 1, and twice with 500 µl Wash Solution 2/3. After a final spin

460 to remove residual ethanol, RNA was eluted with 25 µl 95°C preheated Elution Solution. The
461 elution step was repeated, and eluates combined. RNA was then treated with DNaseI using 6 µl
462 DNaseI buffer and 4 µl DNaseI for 30 min at 37 deg C, then treated with Inactivation Reagent
463 for 5 min at RT. RNA was then biotinylated essentially as described (Duffy et al., 2015; Duffy and
464 Simon, 2016) using 40 µl (~40 µg) total RNA and 4 µg MTSEA biotin-XX (Biotium) in the
465 following reaction: 40 µl total 4-thioU-labeled RNA, 20 mM HEPES, 1 mM EDTA, 4 µg MTSEA
466 biotin-XX (80 µl 50 µg/ml diluted stock) in a 400 µl final volume. Biotinylation reactions
467 occurred for 30 min at RT with rotation and under foil. Unreacted MTS-biotin was removed by
468 phenol/$CHCl_3$/IAA extraction. RNA was precipitated with isopropanol and resuspended in 100 µl
469 nuclease-free H_2O. Biotinylated RNA was purified also as described (Duffy and Simon, 2016)
470 using 80 µl MyOne Streptavidin C1 Dynabeads (Invitrogen) + 100 µl biotinylated RNA for 15 min
471 at RT with rotation and under foil. Prior to use, MyOne Streptavidin beads were washed in a
472 single batch with 3X 3 ml H_2O, 3X 3 ml High Salt Wash Buffer (100 mM Tris, 7.4, 10 mM EDTA, 1
473 M NaCl, 0.05% Tween-20), blocked in 4 ml High Salt Wash Buffer containing 40 ng/µl glycogen
474 for 1 hour at RT, then resuspended to the original volume in High Salt Wash Buffer. After
475 incubation with biotinylated RNA, the beads were washed 3X 0.8 ml High Salt Wash Buffer,
476 then eluted into 25 µl streptavidin elution buffer (100 mM DTT, 20 mM HEPES 7.4, 1 mM EDTA,
477 100 mM NaCl, 0.05% Tween-20) at RT with shaking, then the elution step repeated and
478 combined for a total of 50 µl. At this point, 10% input RNA (4 µl) was diluted into 50 µl
479 streptavidin elution buffer and processed the same as the labeled RNA samples to determine
480 the extent of recovery. 50 µl each input and purified RNA was adjusted to 100 µl with nuclease-
481 free water and purified on RNeasy columns (Qiagen) using the modified protocol as described
482 (Duffy and Simon, 2016). To each 100 µl sample, 350 µl RLT (supplemented with 10 µl 1% ME
483 per 1 ml RLT) and 250 µl 100% ethanol was added, mixed well, and applied to columns.
484 Columns were washed with 500 µl RPE (supplemented 35 µl 1% ME per 500 µl RPE), followed
485 by a final 5 min spin at max speed. RNAs were eluted into 14 µl nuclease-free water.
486
487 **cDNA Synthesis and Quantitative PCR of newly-synthesized RNA**

488 Two microliters RNA was used to generate cDNA using Transcriptor (Roche), random hexamer
489 primer, and the manufacturer's instructions. cDNA was used either undiluted, 1/20, or 1/100
490 for quantitative PCR (qPCR) depending on the gene analyzed. Gene-specific qPCR was
491 performed in triplicate using primers near the 5' end of the gene. qPCRs were assembled in 5 µl
492 reaction mixtures in a 384-well plate using 2X Power SYBR green master mix (Thermo Fisher
493 Scientific) and reactions were run on the QuantStudio5 Real-Time System (Thermo Fisher
494 Scientific). Relative amounts of DNA were calculated using a standard curve generated from 10-
495 fold serial dilutions of purified genomic DNA ranging from 10 ng to 0.001 ng. Relative amounts
496 of *S. cerevisiae* transcript were normalized to *S. pombe* tubulin transcripts. All values are
497 expressed relative to that of either wild type +SM or the Spt3/7-deg +SM strain, which were set
498 to 1.0. Each experiment was performed in two biological replicates (cultures collected on
499 separate days) and three technical replicates (independent measurements of the same qPCR
500 sample). Values for technical replicates were averaged which gave a single value for each
501 biological replicate. The final result is a mean of biological replicates.
502
503
504 **Preparation of 4ThioU RNA Libraries for NGS**
505 Newly synthesized RNA isolated via 4-thioU labeling and purification was prepared for
506 sequencing using the Ovation SoLo or Ovation Universal RNA-seq System kits (Tecan) according
507 to the manufacturer's instructions and 1 ng (SoLo) or 50 ng (Universal) input RNA. Libraries
508 were sequenced on the Illumina HiSeq2500 platform using 25 bp paired-ends at the Fred
509 Hutchinson Genomics Shared Resources facility.
510
511 **ChEC-seq experiments and library preparation**
512 ChEC-seq experiments were performed in four replicates as described (Donczew et al.,
513 submitted.). Libraries were prepared as described (Donczew et al., submitted) and sequenced
514 on the Illumina HiSeq2500 platform using 25 bp paired-ends at the Fred Hutchinson Genomics
515 Shared Resources facility.
516

517 **Western Blot Analysis**

518 1 ml cell culture was collected and pelleted from strains after treatment with 3IAA or DMSO,
519 washed with 500 μl water, then resuspended in 75 μl yeast whole cell extract buffer. After
520 heating for 5 min at 95 deg, samples were centrifuged for 5 min at max speed, whole cell
521 extracts were separated by SDS-PAGE and analyzed by Western blot using mouse monoclonal
522 or rabbit polyclonal antibodies. Protein signals were visualized by using the Odyssey CLx
523 scanner and quantified using Odyssey Image Studio software (Li-Cor) by generating a standard
524 curve using a titration from WT extract. Each protein analyzed was normalized to the amount of
525 the TFIIF subunit Tfg2. H2B-Ub was probed with antibody 5546 (Cell Signaling Technology) and
526 H3K18-Ac with antibody 07-354 from EMD Millipore.

527

528 **Analysis of RNA-Seq Data**

529 The majority of the data analysis tasks except sequence alignment and reads counting
530 (described below) was performed through interactive work in the Jupyter Notebook
531 (https://jupyter.org) using Python programming language (https://www.python.org) and short
532 Bash scripts. All figures were generated using Matplotlib and Seaborn libraries for Python
533 ((Hunter, 2007); https://matplotlib.org; https://seaborn.pydata.org). All code snippets and
534 whole notebooks are available upon request.

535

536 Paired-end sequencing reads were aligned to *S. cerevisiae* reference genome (sacCer3) and *S.*
537 *pombe* reference genome (ASM294v2.20) with Bowtie2 (Langmead and Salzberg, 2012) using
538 optional arguments "-I 10 -X 700 --local --very-sensitive-local --no-unal --no-mixed --no-
539 discordant". The resulting SAM files for S. cerevisiae data were used as an input for HTseq-
540 count (Anders et al., 2015) with default settings. The GFF file with *S. cerevisiae* genomic
541 features was downloaded from the Ensembl website (assembly R64-1-1). Signal per gene was
542 normalized by the number of all *S. pombe* reads mapped for the sample and multiplied by
543 10000 (arbitrarily chosen number). Genes classified as dubious, pseudogenes or transposable
544 elements were excluded leaving 5797 genes for the downstream analysis. As a next filtering
545 step, we excluded all the genes that had no measurable signal in at least one out of all 48

546 samples (additional 12 samples for simultaneous depletion of SAGA and TFIID were not used for
547 this filtering step). The remaining 5158 genes were sorted by the average expression level
548 based on combined results of all WT and DMSO samples (22 samples total). For this analysis
549 signal per gene was further normalized by the gene length. Results from all relevant samples
550 were averaged and genes were ranked (**Table S1**). We used this information to filter out 258
551 genes with the lowest expression after comparing average coefficient of variation for each
552 sample depending on the number of highly expressed genes left in the analysis. Our final
553 dataset contains 4900 genes which give reproducible results and represent a substantial part of
554 the yeast genome. The results of biological replicate experiments for each sample were
555 averaged (**Table S2**). All experiments were done in triplicate except YPD Taf-degron and wild-
556 type BY4705 samples (labeled SHY772) that were done in duplicate. Replicate experiments
557 showed low variation for the majority of genes which is visualized in **Fig S1** using coefficient of
558 variation. Corresponding samples were compared to calculate $\log_2$ change in expression per
559 gene (IAA to DMSO samples for degron experiments and deletion mutant to WT strain for SAGA
560 deletion experiments – strain BY4705 (Brachmann et al., 1998) was used as a background for
561 *SPT20* and *SPT7* deletion strains, SHY565 (BY4705 with Rpb3-3xFlag::KanMX) was used to
562 construct the *SPT3* deletion strain) and degron strains are derivatives of SHY1037 (Warfield et
563 al., 2017)) (**Table S3**).
564
565 **Analysis of ChEC-seq Data**
566 ChEC-seq data was analyzed as described (Donczew et al., submitted). Briefly, for each replicate
567 peaks were called using the HOMER suite of tools (Heinz et al., 2010) (http://homer.ucsd.edu).
568 Peaks identified by this method were assigned to promoters and for the final list only
569 promoters bound in at least three replicates were included.
570
571 **Data availability**
572 RNA-seq data (GSE133004) and ChEC-seq data (Donczew et al., submitted; GSE133114) has
573 been submitted to GEO and will be available upon peer-reviewed publication.
574

575 **Author contributions**

576 LW and RD performed RNA-seq, RD and AE performed computational analysis and RD, LW and
577 SH designed the study, analyzed the data, and wrote the manuscript.

578

579 **Acknowledgements**

580 We thank Gabe Zentner and Steve Henikoff for discussions, Christine Cucinotta and Brian Strahl
581 for advice on SAGA-regulated chromatin modifications and detection, Wei Sun for discussion
582 regarding clustering approaches, Matthew Fitzgibbon for helpful comments about RNA-seq
583 data analysis and Laszlo Tora, Didier Devys, and Toshi Tsukiyama for comments on the
584 manuscript. Supported by NIH grants GM053451 and GM075114 to SH

585

586 **Table and figure legends**

587 **Figure 1.** Two distinct classes of yeast genes based on SAGA and TFIID dependence. (**A**) Scatter
588 plots comparing normalized signal per gene in corresponding samples. Log_{10} scale is used for X
589 and Y axes. Mean values from replicate experiments are plotted. All presented experiments
590 were done in SC media. (**B**) Box plot showing the log_2 change per gene in depletion
591 experiments. Genes are divided into two classes according to results of the k-means clustering
592 analysis of SAGA deletion and TFIID degron experiments. Two clusters were found to give the
593 best separation using silhouette analysis and log_2 change values from relevant experiments
594 were used as an input for k-means algorithm (KMeans function from Python sklearn.cluster
595 library with default settings).

596

597 **Figure 2.** Simultaneous depletion of SAGA and TFIID severely affects transcription from almost
598 all genes. (**A**) Box plot comparing results of depletion of SAGA or TFIID with simultaneous
599 depletion of both coactivators. Genes are grouped into two categories from Fig 1. All presented
600 experiments were done in SC media. (**B**) Scatter plots comparing results of Taf13-deg and
601 Taf13+Spt3-deg experiments for TFIID/SAGA genes and TFIID genes. Pearson correlation
602 coefficient is shown. (**C**) Scatter plot of gene expression rank vs the difference between the
603 results of Spt3+Taf13-degron experiment and the sum of effects of independent depletions of
604 SAGA and TFIID (Spt3+20-deg and Taf13-deg experiments). Only TFIID/SAGA genes are plotted
605 (655 genes).

606

607 **Figure 3.** The sensitivity of individual genes to TFIID/SAGA depletions is not affected by
608 expression level. (**A**) Bar plot comparing number of genes in two defined classes in expression
609 quintiles (left panel) and among top 10% highly transcribed genes (right panel). (**B**) Scatter plot
610 of average expression vs the gene expression rank. (**C**) Scatter plot comparing gene expression
611 rank with the difference in sensitivity of genes to rapid Taf13 and Spt3+7 depletion. Only
612 TFIID/SAGA genes are plotted (655 genes). (**D**) Number of TFIID and TFIID/SAGA genes among
613 TATA-less and TATA-containing categories. Consensus TATA was defined as TATAWAW and the
614 TATA-element positions from Pugh and colleagues (Rhee and Pugh, 2012) were used.

615

616 **Figure 4.** Histone modifications in *SPT* deletion and degron strains. Western blot of the SAGA-
617 dependent marks H3K18-acetyl and H2B-Ub in (**A**) *SPT* deletions and (**B**) *SPT*-degron strains.
618 Variable amounts of wild-type samples without 3-IAA treatment were loaded to allow
619 quantitation of histone modifications. In panel A, volumes extract loaded: 6, 3, 1.5, 0.75 μl
620 (WT); 12, 6 μl (*spt∆* strains); 6, 2 μl (*ubp8∆*). Histone marks in each sample were normalized to
621 the TFIIF subunit Tfg2. (**C**) Western blot showing degron depletion in *SPT* double degron strains
622 after treatment with 3-IAA for times indicated in panel B. Blots were probed with α-H3K18-Ac,
623 α-H2B-Ub, and α-Tfg2 polyclonal antibodies (**A, B**) or α-V5 monoclonal antibodies (**C**)**.**
624

625 **Figure 5.** Effects of *SPT* deletions or degron-depletion in SM-induced cells. RT-qPCR analysis of
626 4-thio Uracil labeled RNA purified from indicated *SPT* deletion strains in the presence or
627 absence of SM (**A**) or from *SPT*-degron strains induced with SM either before or after treatment
628 with 3-IAA (**B**). Samples were normalized by spike-in of labeled *S. pombe* cells before RNA
629 isolation, and RT qPCR values from each *S. cerevisiae* gene were normalized to the value of the
630 *S. pombe* tubulin gene. Each experiment was performed in two biological and three technical
631 replicates. Error bars represent the standard error of the mean for two biological replicates
632 (values obtained after averaging results for three technical replicates).
633

634 **Figure 6.** TFIID and SAGA show widespread binding to both gene classes. (**A**) Venn-diagram
635 showing extensive overlap between Taf7 and Spt7 bound promoters (Donczew et al.,
636 submitted). (**B**) Number of promoters bound by the indicated subunit of TFIID or SAGA with
637 genes separated into TFIID/SAGA-redundant and TFIID-dependent gene categories.
638

639 **Figure 7. Model for roles of TFIID and SAGA and two different gene classes.** Of the ~83% of
640 yeast protein-coding genes analyzed in this study, the number of genes in each class is shown.
641 Expression of genes in the TFIID set is strongly TFIID-dependent with little or no change after
642 rapid SAGA depletion. TFIID and SAGA both contribute to expression of the TFIID/SAGA genes
643 where these factors have substantial overlapping function as revealed by rapid depletion

644 experiments. Prior work suggests that these effects are due to the TBP-promoter DNA loading
645 functions of TFIID and SAGA. Expression of nearly all genes is dependent on a separate function
646 of SAGA, revealed by deletions in SAGA subunit genes, that is linked to chromatin modifications
647 that change slowly after rapid SAGA depletion.
648
649 **Figure S1** (related to Figs 1 and 2). (**A**) Average coefficients of variation (CV) for selected
650 experiments vs the percentage of genes analyzed (after filtering out 639 genes which did not
651 have RNA-seq signal in at least one experiment). CV values were calculated for each gene based
652 on normalized read counts. **(B**) Gene-specific coefficients of variation (CV) for all 4-thioU RNA-
653 seq experiments. All samples were done in triplicate except the YPD-grown cultures: Taf-degron
654 and wild-type BY4705 samples (labeled SHY772) that were done in duplicate. CV values were
655 calculated for each gene based on normalized read counts for replicate experiments. (**C)**
656 Correlation matrix of Pearson correlation coefficient values between $\log_2$ changes in
657 transcription in all SAGA and TFIID depletion experiments.
658
659 **Figure S2** (related to Figs 1 and 2). (**A**) Degron depletion in single or double degron strains.
660 Western blot showing degron efficiency in cells grown in synthetic complete media. Experiment
661 was done in biological triplicates (A, B, and C cultures – top panel) or biological duplicates (one
662 replicate shown, panel B). Variable amounts of the untreated samples were loaded to allow
663 quantitation of degron efficiency. Blots were probed with α-V5 monoclonal (Spt20, Spt3, Spt7,
664 Taf13, Taf1, Taf7-degrons) or α-Tfg2 polyclonal antibodies. (**B**) Western analysis of TFIID
665 subunits in Taf-degron strains grown in YPD.
666
667 **Figure S3** (related to Fig 3). (A) Barplot comparing previously proposed categories (Huisinga and
668 Pugh, 2004) with categories defined in this study. (**B**) Scatter plots of $\log_2$ change in
669 transcription in the indicated experiments vs the gene rank based on average expression
670 values. Dots are color-coded based on gene category. (**C**) Boxplot representation of average
671 expression per gene in expression quintiles based on 4thioU RNA labeling.
672

673 **Figure S4** (related to Fig 3). Number of RP genes within each expression quintile.

674

675 **Figure S5 (**related to Fig 5). Degron efficiency in synthetic complete media with or without SM
676 induction and Auxin addition. (**A**) Western analysis of the Spt3 + Spt7-degron strain without SM
677 and with or without 3-IAA. (**B**) Western analysis of the Spt3 + Spt7-degron strain treated with
678 SM either before or after 3-IAA addition. Blot was probed with α-V5 antibody (degron-tagged
679 proteins) and α-Tfg2 as control.

680

681 **Table S1.** Normalized signal for all genes (5158) which had detectable transcription in all 48
682 RNA-seq samples collected in this study (excluding degron experiments simultaneously
683 depleting SAGA and TFIID subunits). Expression is the average signal for all DMSO and WT
684 samples. This value was further normalized by the gene length to give normalized expression
685 which was used to sort the genes from the highest to the lowest expression.

686

687 **Table S2.** Average normalized signal for replicate experiments for the final set of 4900 genes
688 analyzed in this study and average expression per gene (based on DMSO and WT experiments).
689 Rows are sorted by the average expression.

690

691 **Table S3.** Average $\log_2$ changes in transcription in the degron and deletion strains, results of k-
692 means clustering and average expression per gene (based on DMSO and WT experiments).
693 Rows are sorted by the average expression.

694

695 **Table S4**. Average $\log_2$ changes in transcription from degron experiments simultaneously
696 depleting SAGA and TFIID components. Data for other strains, results of k-means clustering and
697 average expression per gene are the same as shown in table S3. Rows are sorted by the average
698 expression.

699 **References**

700 Allen, B.L., Taatjes, D.J., 2015. The Mediator complex: a central integrator of transcription. Nat
701 Rev Mol Cell Biol 16, 155–166. doi:10.1038/nrm3951
702 Anders, S., Pyl, P.T., Huber, W., 2015. HTSeq--a Python framework to work with high-
703 throughput sequencing data. Bioinformatics 31, 166–169.
704 doi:10.1093/bioinformatics/btu638
705 Baptista, T., Grünberg, S., Minoungou, N., Koster, M.J.E., Timmers, H.T.M., Hahn, S., Devys, D.,
706 Tora, L., 2017. SAGA Is a General Cofactor for RNA Polymerase II Transcription. Mol Cell 68,
707 130–143.e5. doi:10.1016/j.molcel.2017.08.016
708 Basehoar, A.D., Zanton, S.J., Pugh, B.F., 2004. Identification and distinct regulation of yeast
709 TATA box-containing genes. Cell 116, 699–709.
710 Bhaumik, S.R., Green, M.R., 2001. SAGA is an essential in vivo target of the yeast acidic activator
711 Gal4p. Genes Dev 15, 1935–1945. doi:10.1101/gad.911401
712 Bieniossek, C., Papai, G., Schaffitzel, C., Garzoni, F., Chaillet, M., Scheer, E., Papadopoulos, P.,
713 Tora, L., Schultz, P., Berger, I., 2013. The architecture of human general transcription factor
714 TFIID core complex. Nature 493, 699–702. doi:10.1038/nature11791
715 Bonnet, J., Wang, C.-Y., Baptista, T., Vincent, S.D., Hsiao, W.-C., Stierle, M., Kao, C.-F., Tora, L.,
716 Devys, D., 2014. The SAGA coactivator complex acts on the whole transcribed genome and
717 is required for RNA polymerase II transcription. Genes Dev 28, 1999–2012.
718 doi:10.1101/gad.250225.114
719 Brachmann, C.B., Davies, A., Cost, G.J., Caputo, E., Li, J., Hieter, P., Boeke, J.D., 1998. Designer
720 deletion strains derived from Saccharomyces cerevisiae S288C: a useful set of strains and
721 plasmids for PCR-mediated gene disruption and other applications. Yeast 14, 115–132.
722 doi:10.1002/(SICI)1097-0061(19980130)14:2<115::AID-YEA204>3.0.CO;2-2
723 Chan, L.Y., Mugler, C.F., Heinrich, S., Vallotton, P., Weis, K., 2018. Non-invasive measurement of
724 mRNA decay reveals translation initiation as the major determinant of mRNA stability. eLife
725 7, 2433. doi:10.7554/eLife.32536
726 Daniel, J.A., Torok, M.S., Sun, Z.-W., Schieltz, D., Allis, C.D., Yates, J.R., Grant, P.A., 2004.
727 Deubiquitination of histone H2B by a yeast acetyltransferase complex regulates
728 transcription. J Biol Chem 279, 1867–1871. doi:10.1074/jbc.C300494200
729 Donczew, R., Hahn, S., 2018. Mechanistic Differences in Transcription Initiation at TATA-Less
730 and TATA-Containing Promoters. Mol Cell Biol 38. doi:10.1128/MCB.00448-17
731 Donczew, R., Lalou, A., Pacheco, D., Devys, D., Tora, L., Hahn, S., n.d. Widespread binding of
732 TFIID and SAGA to yeast promoters mapped by an improved ChEC-seq method Submitted.
733 Doyon, Y., Côté, J., 2004. The highly conserved and multifunctional NuA4 HAT complex. Curr
734 Opin Genet Dev 14, 147–154. doi:10.1016/j.gde.2004.02.009
735 Dudley, A.M., Rougeulle, C., Winston, F., 1999. The Spt components of SAGA facilitate TBP
736 binding to a promoter at a post-activator-binding step in vivo. Genes Dev 13, 2940–2945.
737 Duffy, E.E., Rutenberg-Schoenberg, M., Stark, C.D., Kitchen, R.R., Gerstein, M.B., Simon, M.D.,
738 2015. Tracking Distinct RNA Populations Using Efficient and Reversible Covalent Chemistry.
739 Mol Cell 59, 858–866. doi:10.1016/j.molcel.2015.07.023
740 Duffy, E.E., Simon, M.D., 2016. Enriching s(4) U-RNA Using Methane Thiosulfonate (MTS)
741 Chemistry. Curr Protoc Chem Biol 8, 234–250. doi:10.1002/cpch.12

742 Grant, P.A., Schieltz, D., Pray-Grant, M.G., Steger, D.J., Reese, J.C., Yates, J.R., Workman, J.L.,
743 1998. A subset of TAF(II)s are integral components of the SAGA complex required for
744 nucleosome acetylation and transcriptional stimulation. Cell 94, 45–53.
745 Grünberg, S., Henikoff, S., Hahn, S., Zentner, G.E., 2016. Mediator binding to UASs is broadly
746 uncoupled from transcription and cooperative with TFIID recruitment to promoters. EMBO
747 J 35, 2435–2446. doi:10.15252/embj.201695020
748 Hahn, S., Young, E.T., 2011. Transcriptional regulation in Saccharomyces cerevisiae:
749 transcription factor regulation and function, mechanisms of initiation, and roles of
750 activators and coactivators. Genetics 189, 705–736. doi:10.1534/genetics.111.127019
751 Haimovich, G., Medina, D.A., Causse, S.Z., Garber, M., Millán-Zambrano, G., Barkai, O., Chávez,
752 S., Pérez-Ortín, J.E., Darzacq, X., Choder, M., 2013. Gene expression is circular: factors for
753 mRNA degradation also foster mRNA synthesis. Cell 153, 1000–1011.
754 doi:10.1016/j.cell.2013.05.012
755 Han, Y., Luo, J., Ranish, J., Hahn, S., 2014. Architecture of the Saccharomyces cerevisiae SAGA
756 transcription coactivator complex. EMBO J 33, 2534–2546. doi:10.15252/embj.201488638
757 Hantsche, M., Cramer, P., 2017. Conserved RNA polymerase II initiation complex structure. Curr
758 Opin Struct Biol 47, 17–22. doi:10.1016/j.sbi.2017.03.013
759 Heinz, S., Benner, C., Spann, N., Bertolino, E., Lin, Y.C., Laslo, P., Cheng, J.X., Murre, C., Singh, H.,
760 Glass, C.K., 2010. Simple combinations of lineage-determining transcription factors prime
761 cis-regulatory elements required for macrophage and B cell identities. Mol Cell 38, 576–
762 589. doi:10.1016/j.molcel.2010.05.004
763 Helmlinger, D., Marguerat, S., Villén, J., Swaney, D.L., Gygi, S.P., Bähler, J., Winston, F., 2011.
764 Tra1 has specific regulatory roles, rather than global functions, within the SAGA co-
765 activator complex. EMBO J 30, 2843–2852. doi:10.1038/emboj.2011.181
766 Henry, K.W., Wyce, A., Lo, W.-S., Duggan, L.J., Emre, N.C.T., Kao, C.-F., Pillus, L., Shilatifard, A.,
767 Osley, M.A., Berger, S.L., 2003. Transcriptional activation via sequential histone H2B
768 ubiquitylation and deubiquitylation, mediated by SAGA-associated Ubp8. Genes Dev 17,
769 2648–2663. doi:10.1101/gad.1144003
770 Huisinga, K.L., Pugh, B.F., 2004. A genome-wide housekeeping role for TFIID and a highly
771 regulated stress-related role for SAGA in Saccharomyces cerevisiae. Mol Cell 13, 573–585.
772 Joo, Y.J., Ficarro, S.B., Soares, L.M., Chun, Y., Marto, J.A., Buratowski, S., 2017. Downstream
773 promoter interactions of TFIID TAFs facilitate transcription reinitiation. Genes Dev 31,
774 2162–2174. doi:10.1101/gad.306324.117
775 Kamenova, I., Warfield, L., Hahn, S., 2014. Mutations on the DNA binding surface of TBP
776 discriminate between yeast TATA and TATA-less gene transcription. Mol Cell Biol 34, 2929–
777 2943. doi:10.1128/MCB.01685-13
778 Kolesnikova, O., Ben-Shem, A., Luo, J., Ranish, J., Schultz, P., Papai, G., 2018. Molecular
779 structure of promoter-bound yeast TFIID. Nat Commun 9, 4666. doi:10.1038/s41467-018-
780 07096-y
781 Koutelou, E., Hirsch, C.L., Dent, S.Y.R., 2010. Multiple faces of the SAGA complex. Curr. Opin.
782 Cell Biol. 22, 374–382. doi:10.1016/j.ceb.2010.03.005
783 Kuras, L., Kosa, P., Mencia, M., Struhl, K., 2000. TAF-Containing and TAF-independent forms of
784 transcriptionally active TBP in vivo. Science 288, 1244–1248.

785 Langmead, B., Salzberg, S.L., 2012. Fast gapped-read alignment with Bowtie 2. Nat Meth 9,
786 357–359. doi:10.1038/nmeth.1923
787 Laprade, L., Rose, D., Winston, F., 2007. Characterization of new Spt3 and TATA-binding protein
788 mutants of Saccharomyces cerevisiae: Spt3 TBP allele-specific interactions and bypass of
789 Spt8. Genetics 177, 2007–2017. doi:10.1534/genetics.107.081976
790 Lee, K.K., Sardiu, M.E., Swanson, S.K., Gilmore, J.M., Torok, M., Grant, P.A., Florens, L.,
791 Workman, J.L., Washburn, M.P., 2011. Combinatorial depletion analysis to assemble the
792 network architecture of the SAGA and ADA chromatin remodeling complexes. Molecular
793 Systems Biology 7, 503. doi:10.1038/msb.2011.40
794 Lee, T.I., Causton, H.C., Holstege, F.C., Shen, W.C., Hannett, N., Jennings, E.G., Winston, F.,
795 Green, M.R., Young, R.A., 2000. Redundant roles for the TFIID and SAGA complexes in
796 global transcription. Nature 405, 701–704. doi:10.1038/35015104
797 Li, X.Y., Bhaumik, S.R., Green, M.R., 2000. Distinct classes of yeast promoters revealed by
798 differential TAF recruitment. Science 288, 1242–1244.
799 Liu, G., Zheng, X., Guan, H., Cao, Y., Qu, H., Kang, J., Ren, X., Lei, J., Dong, M.-Q., Li, X., Li, H.,
800 2019. Architecture of Saccharomyces cerevisiae SAGA complex. Cell Discov 5, 25.
801 doi:10.1038/s41421-019-0094-x
802 Louder, R.K., He, Y., López-Blanco, J.R., Fang, J., Chacón, P., Nogales, E., 2016. Structure of
803 promoter-bound TFIID and model of human pre-initiation complex assembly. Nature 531,
804 604–609. doi:10.1038/nature17394
805 Mohibullah, N., Hahn, S., 2008. Site-specific cross-linking of TBP in vivo and in vitro reveals a
806 direct functional interaction with the SAGA subunit Spt3. Genes Dev 22, 2994–3006.
807 doi:10.1101/gad.1724408
808 Moqtaderi, Z., Bai, Y., Poon, D., Weil, P.A., Struhl, K., 1996. TBP-associated factors are not
809 generally required for transcriptional activation in yeast. Nature 383, 188–191.
810 doi:10.1038/383188a0
811 Morris, S.A., Rao, B., Garcia, B.A., Hake, S.B., Diaz, R.L., Shabanowitz, J., Hunt, D.F., Allis, C.D.,
812 Lieb, J.D., Strahl, B.D., 2007. Identification of histone H3 lysine 36 acetylation as a highly
813 conserved histone modification. J Biol Chem 282, 7632–7640. doi:10.1074/jbc.M607909200
814 Munchel, S.E., Shultzaberger, R.K., Takizawa, N., Weis, K., 2011. Dynamic profiling of mRNA
815 turnover reveals gene-specific and system-wide regulation of mRNA decay. Molecular
816 Biology of the Cell 22, 2787–2795. doi:10.1091/mbc.E11-01-0028
817 Nishimura, K., Fukagawa, T., Takisawa, H., Kakimoto, T., Kanemaki, M., 2009. An auxin-based
818 degron system for the rapid depletion of proteins in nonplant cells. Nat Meth 6, 917–922.
819 doi:10.1038/nmeth.1401
820 Nogales, E., Fang, J., Louder, R.K., 2017a. Structural dynamics and DNA interaction of human
821 TFIID. transcription 8, 55–60. doi:10.1080/21541264.2016.1265701
822 Nogales, E., Louder, R.K., He, Y., 2017b. Structural Insights into the Eukaryotic Transcription
823 Initiation Machinery. Annual review of biophysics 46, 59–83. doi:10.1146/annurev-biophys-
824 070816-033751
825 Patel, A.B., Louder, R.K., Greber, B.J., Grünberg, S., Luo, J., Fang, J., Liu, Y., Ranish, J., Hahn, S.,
826 Nogales, E., 2018. Structure of human TFIID and mechanism of TBP loading onto promoter
827 DNA. Science 362, eaau8872. doi:10.1126/science.aau8872

828 Petrenko, N., Jin, Y., Dong, L., Wong, K.H., Struhl, K., 2019. Requirements for RNA polymerase II
829 preinitiation complex formation in vivo. eLife 8, 699. doi:10.7554/eLife.43654
830 Rando, O.J., Winston, F., 2012. Chromatin and transcription in yeast. Genetics 190, 351–387.
831 doi:10.1534/genetics.111.132266
832 Rhee, H.S., Pugh, B.F., 2012. Genome-wide structure and organization of eukaryotic pre-
833 initiation complexes. Nature 483, 295–301. doi:10.1038/nature10799
834 Rodriguez-Navarro, S., 2009. Insights into SAGA function during gene expression. EMBO Rep 10,
835 843–850. doi:10.1038/embor.2009.168
836 Sainsbury, S., Bernecky, C., Cramer, P., 2015. Structural basis of transcription initiation by RNA
837 polymerase II. Nat Rev Mol Cell Biol 16, 129–143. doi:10.1038/nrm3952
838 Sermwittayawong, D., Tan, S., 2006. SAGA binds TBP via its Spt8 subunit in competition with
839 DNA: implications for TBP recruitment. EMBO J 25, 3791–3800.
840 doi:10.1038/sj.emboj.7601265
841 Setiaputra, D., Ross, J.D., Lu, S., Cheng, D.T., Dong, M.-Q., Yip, C.K., 2015. Conformational
842 flexibility and subunit arrangement of the modular yeast Spt-Ada-Gcn5 acetyltransferase
843 complex. Journal of Biological Chemistry 290, 10057–10070. doi:10.1074/jbc.M114.624684
844 Sprouse, R.O., Shcherbakova, I., Cheng, H., Jamison, E., Brenowitz, M., Auble, D.T., 2008.
845 Function and structural organization of Mot1 bound to a natural target promoter. J Biol
846 Chem 283, 24935–24948. doi:10.1074/jbc.M803749200
847 Sterner, D.E., Grant, P.A., Roberts, S.M., Duggan, L.J., Belotserkovskaya, R., Pacella, L.A.,
848 Winston, F., Workman, J.L., Berger, S.L., 1999. Functional organization of the yeast SAGA
849 complex: distinct components involved in structural integrity, nucleosome acetylation, and
850 TATA-binding protein interaction. Mol Cell Biol 19, 86–98.
851 Sun, M., Schwalb, B., Schulz, D., Pirkl, N., Etzold, S., Larivière, L., Maier, K.C., Seizl, M., Tresch, A.,
852 Cramer, P., 2012. Comparative dynamic transcriptome analysis (cDTA) reveals mutual
853 feedback between mRNA synthesis and degradation. Genome Res 22, 1350–1359.
854 doi:10.1101/gr.130161.111
855 Tourigny, J.P., Saleh, M.M., Schumacher, K., Devys, D., Zentner, G.E., 2018. Mediator Is Essential
856 for Small Nuclear and Nucleolar RNA Transcription in Yeast. Mol Cell Biol 38.
857 doi:10.1128/MCB.00296-18
858 Walker, S.S., Reese, J.C., Apone, L.M., Green, M.R., 1996. Transcription activation in cells lacking
859 TAFIIS. Nature 383, 185–188. doi:10.1038/383185a0
860 Warfield, L., Ramachandran, S., Baptista, T., Devys, D., Tora, L., Hahn, S., 2017. Transcription of
861 Nearly All Yeast RNA Polymerase II-Transcribed Genes Is Dependent on Transcription Factor
862 TFIID. Mol Cell 68, 118–129.e5. doi:10.1016/j.molcel.2017.08.014
863 Weake, V.M., Workman, J.L., 2008. Histone ubiquitination: triggering gene activity. Mol Cell 29,
864 653–663. doi:10.1016/j.molcel.2008.02.014
865

A

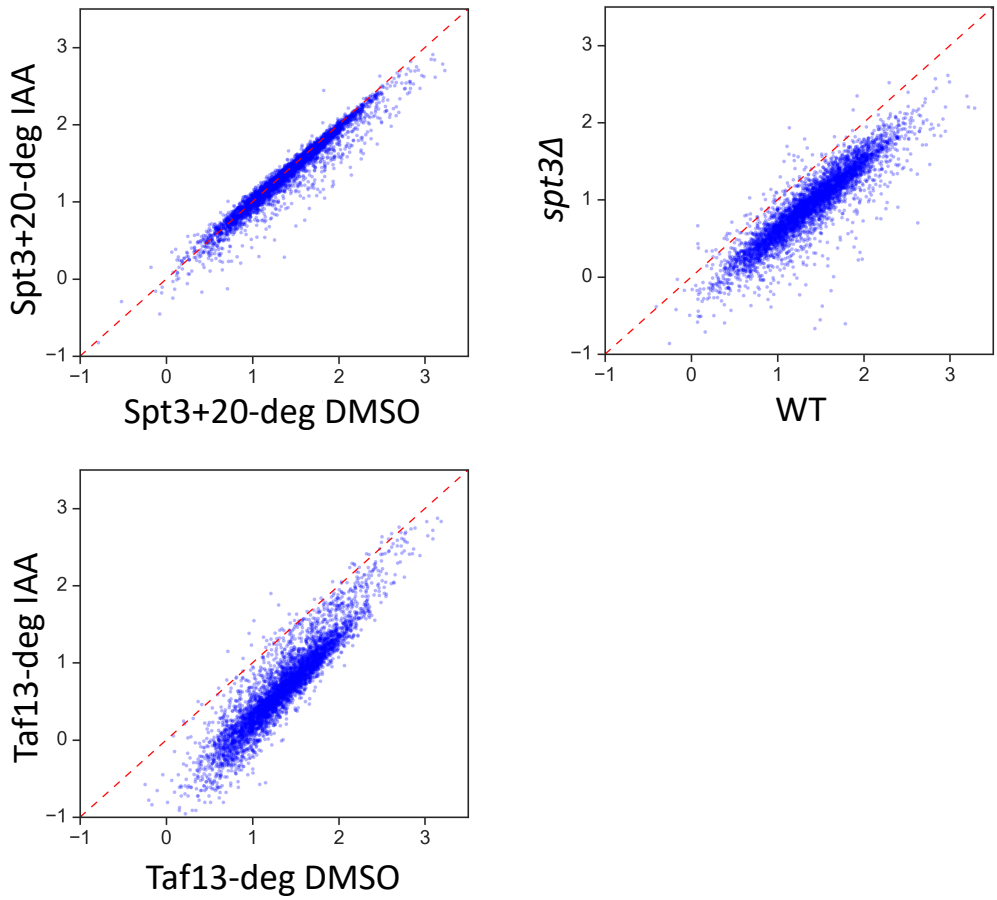
Spt3+20-deg IAA
Spt3+20-deg DMSO
spt3Δ
WT
Taf13-deg IAA
Taf13-deg DMSO

B

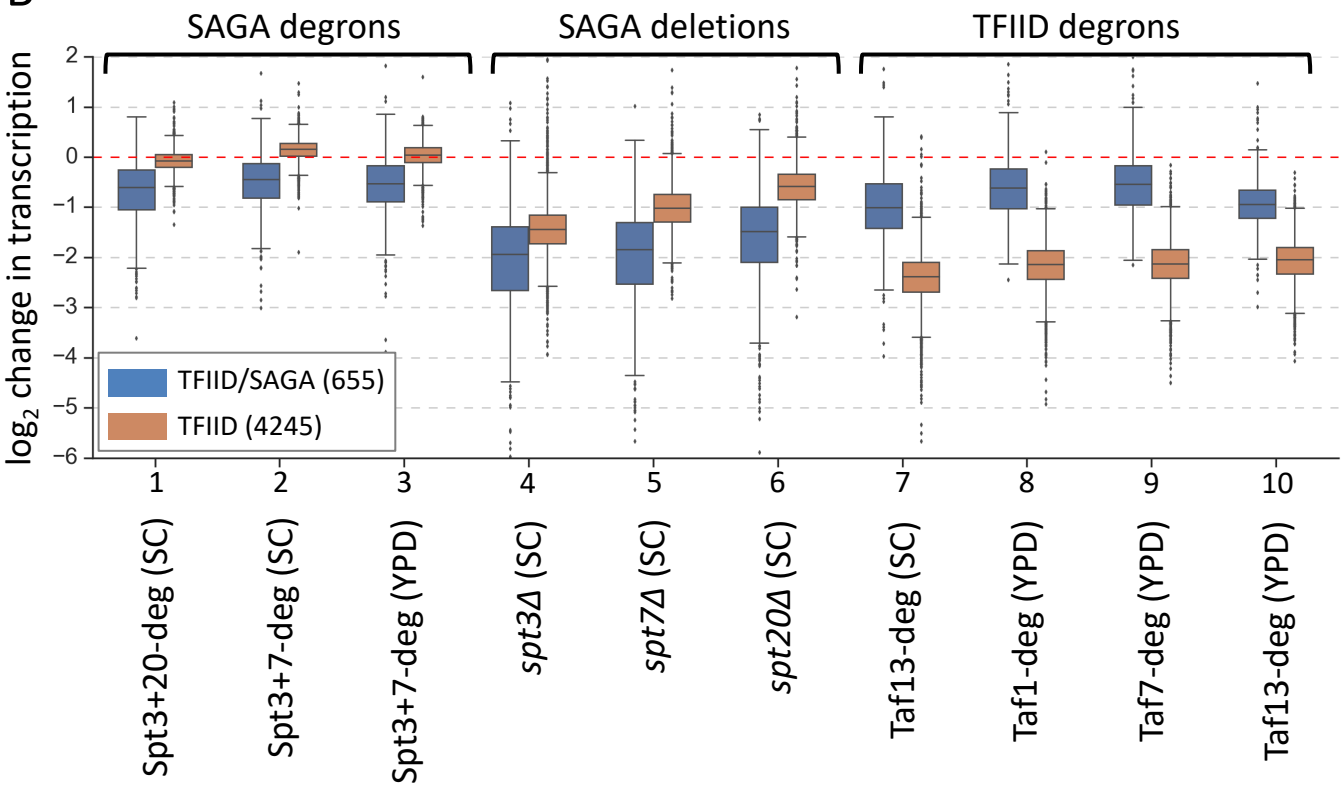
SAGA degrons
SAGA deletions
TFIID degrons
log2 change in transcription
TFIID/SAGA (655)
TFIID (4245)
1 Spt3+20-deg (SC)
2 Spt3+7-deg (SC)
3 Spt3+7-deg (YPD)
4 spt3Δ (SC)
5 spt7Δ (SC)
6 spt20Δ (SC)
7 Taf13-deg (SC)
8 Taf1-deg (YPD)
9 Taf7-deg (YPD)
10 Taf13-deg (YPD)

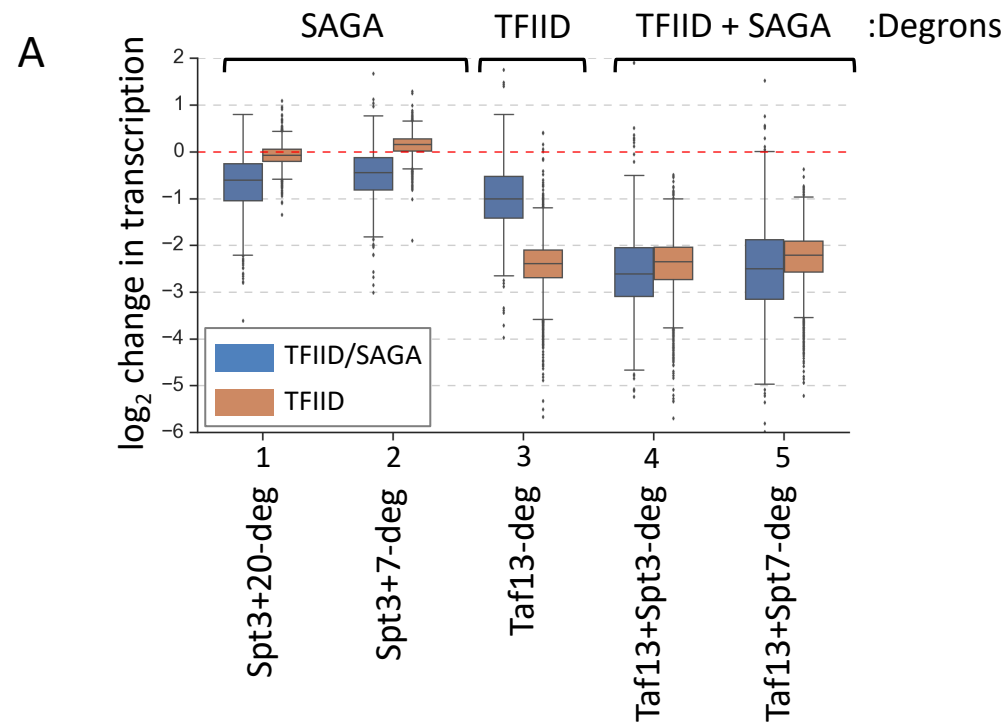
A
SAGA
TFIID
TFIID + SAGA
:Degrons
log2 change in transcription
TFIID/SAGA
TFIID
1
2
3
4
5
Spt3+20-deg
Spt3+7-deg
Taf13-deg
Taf13+Spt3-deg
Taf13+Spt7-deg

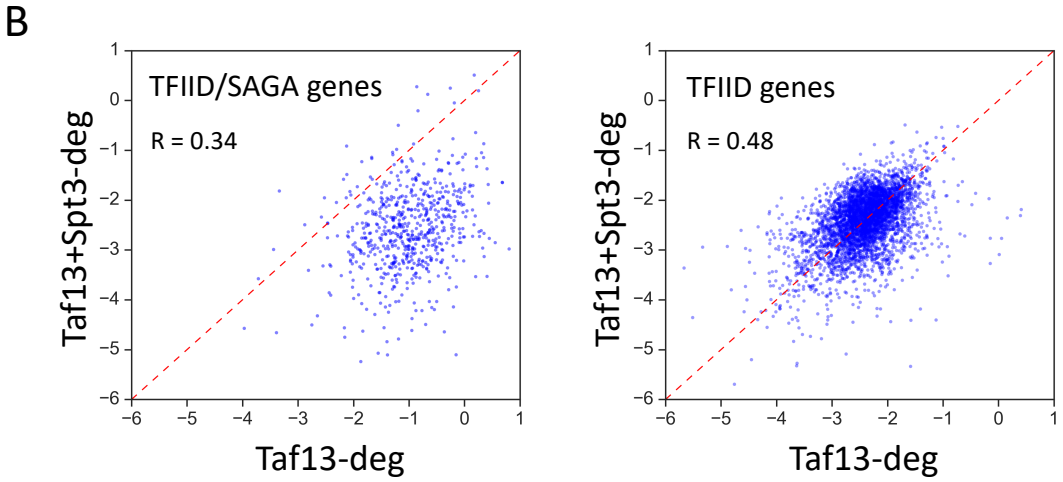
B
TFIID/SAGA genes
R = 0.34
TFIID genes
R = 0.48
Taf13+Spt3-deg
Taf13-deg

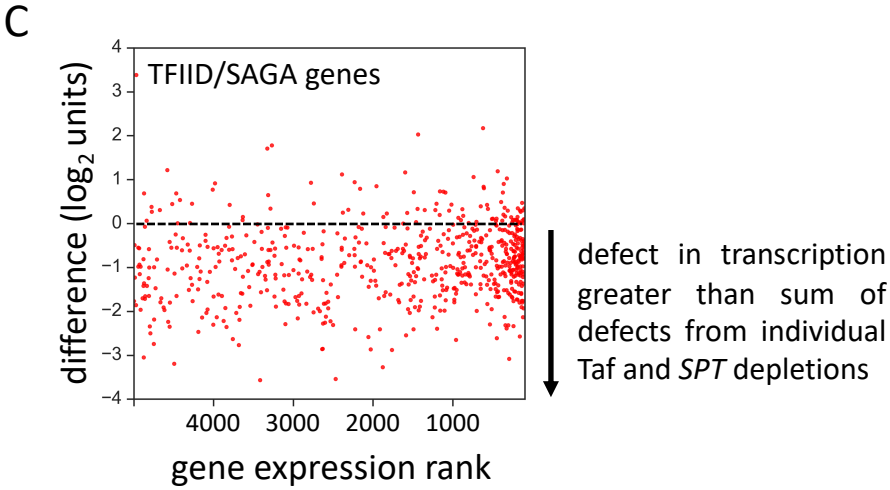
C
TFIID/SAGA genes
difference (log2 units)
gene expression rank
defect in transcription greater than sum of defects from individual Taf and SPT depletions

A

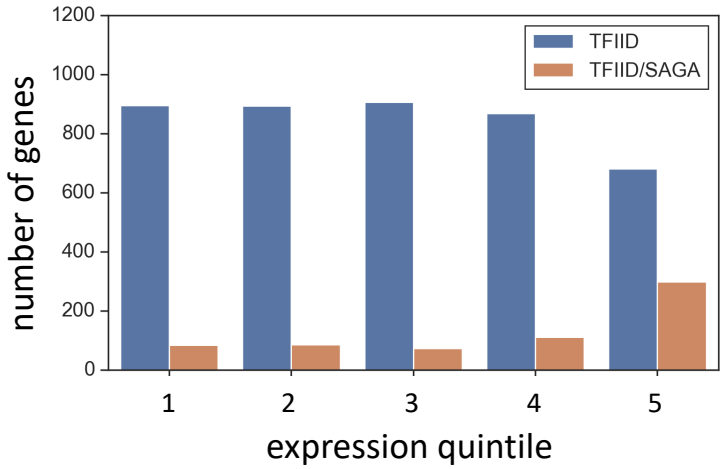

Top 10% transcribed

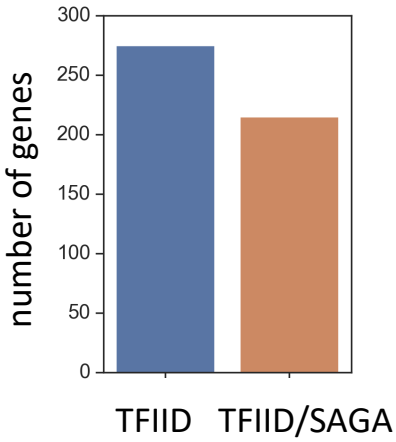

B

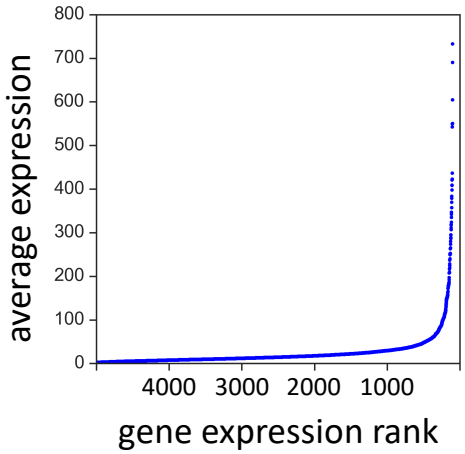

C

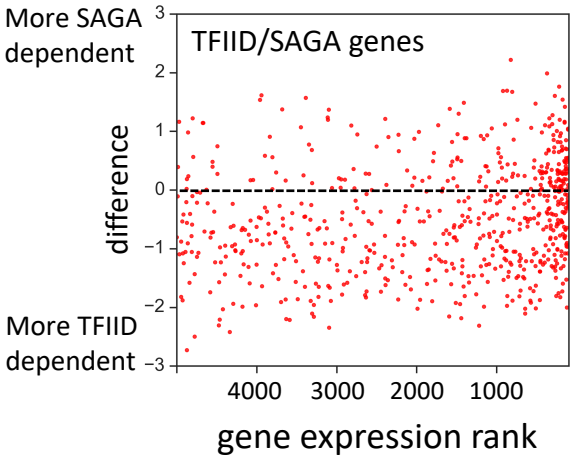

D

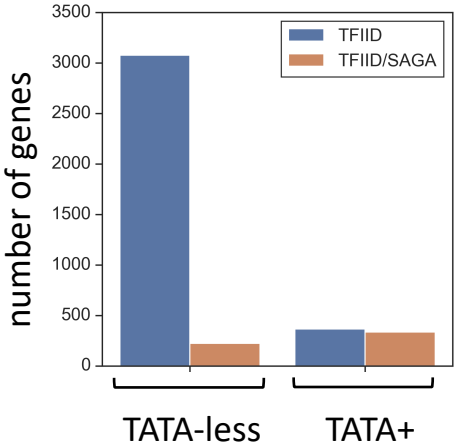

TATA = (TATAWAW)

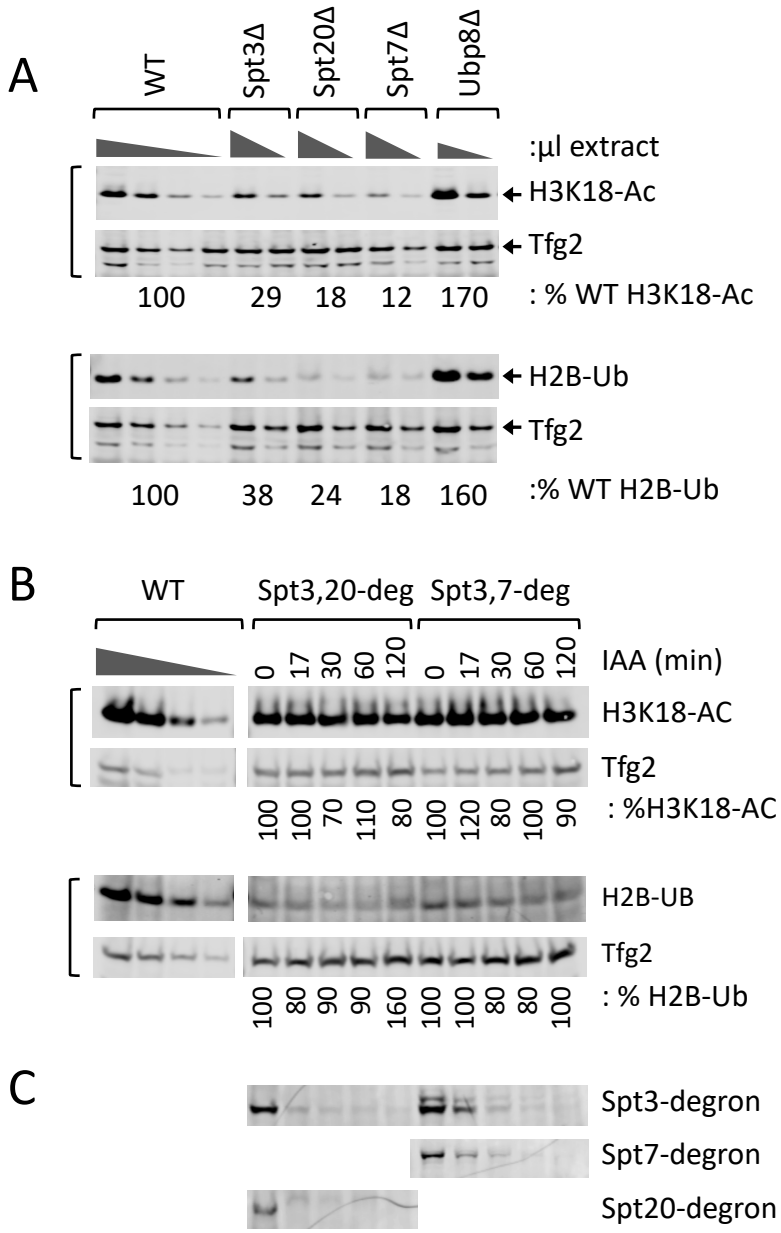
A
WT
Spt3Δ
Spt20Δ
Spt7Δ
Ubp8Δ
:µl extract
H3K18-Ac
Tfg2
100 29 18 12 170
: % WT H3K18-Ac
H2B-Ub
Tfg2
100 38 24 18 160
:% WT H2B-Ub
B
WT
Spt3,20-deg
Spt3,7-deg
0 17 30 60 120 0 17 30 60 120
IAA (min)
H3K18-AC
Tfg2
100 100 70 110 80 100 120 80 100 90
: %H3K18-AC
H2B-UB
Tfg2
100 80 90 90 160 100 100 80 80 100
: % H2B-Ub
C
Spt3-degron
Spt7-degron
Spt20-degron

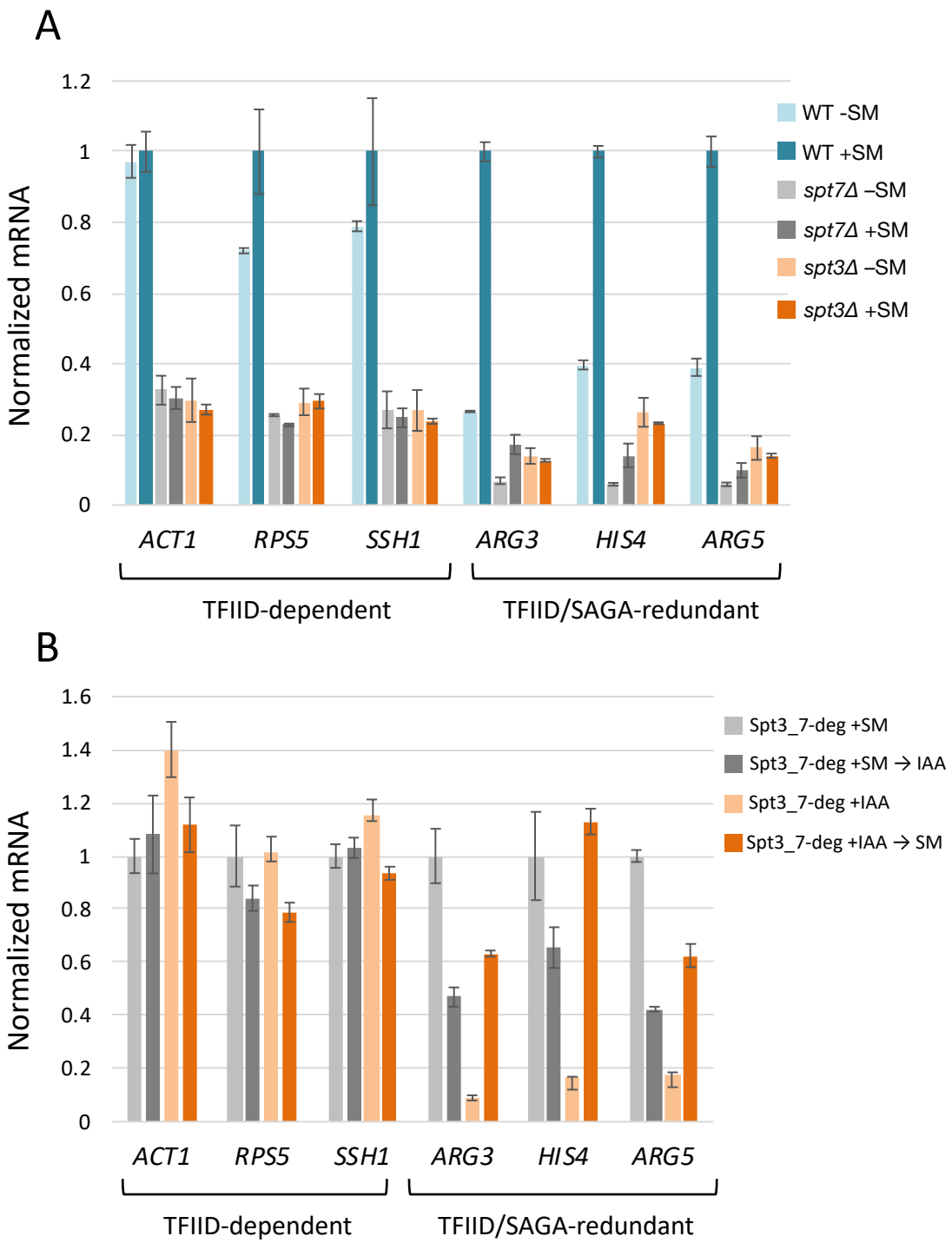
A
Normalized mRNA
1.2
1
0.8
0.6
0.4
0.2
0
WT -SM
WT +SM
spt7Δ –SM
spt7Δ +SM
spt3Δ –SM
spt3Δ +SM
ACT1
RPS5
SSH1
ARG3
HIS4
ARG5
TFIID-dependent
TFIID/SAGA-redundant
B
Normalized mRNA
1.6
1.4
1.2
1
0.8
0.6
0.4
0.2
0
Spt3_7-deg +SM
Spt3_7-deg +SM → IAA
Spt3_7-deg +IAA
Spt3_7-deg +IAA → SM
ACT1
RPS5
SSH1
ARG3
HIS4
ARG5
TFIID-dependent
TFIID/SAGA-redundant

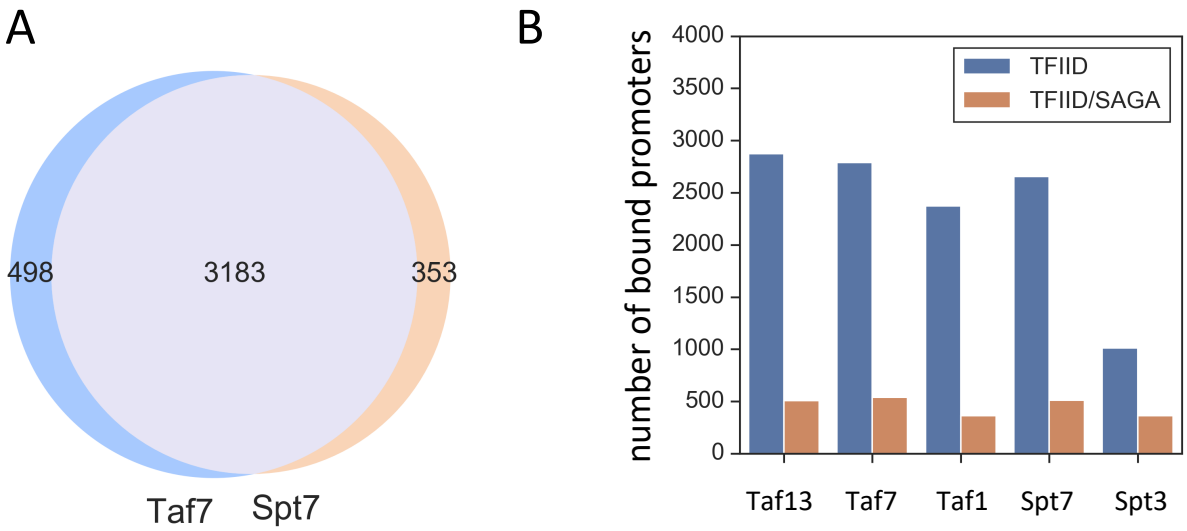
A
498
3183
353
Taf7
Spt7
B
number of bound promoters
4000
3500
3000
2500
2000
1500
1000
500
0
TFIID
TFIID/SAGA
Taf13
Taf7
Taf1
Spt7
Spt3

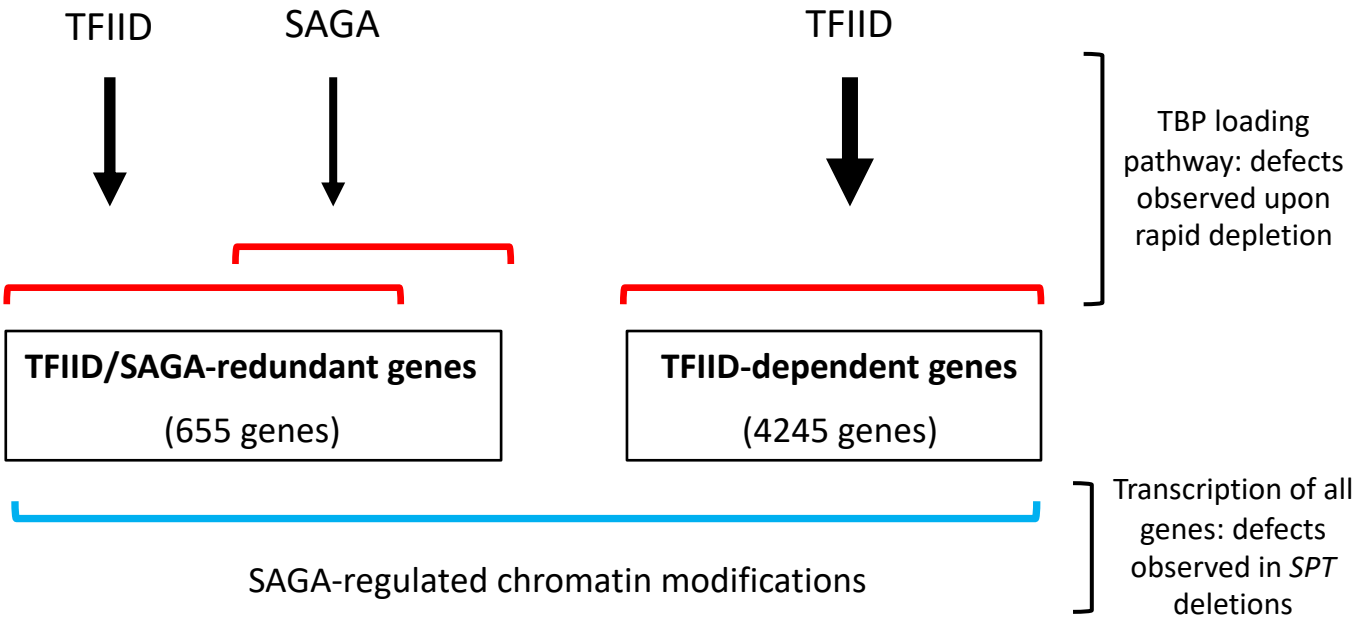
TFIID
SAGA
TFIID
TBP loading pathway: defects observed upon rapid depletion
TFIID/SAGA-redundant genes
(655 genes)
TFIID-dependent genes
(4245 genes)
Transcription of all genes: defects observed in *SPT* deletions
SAGA-regulated chromatin modifications

A

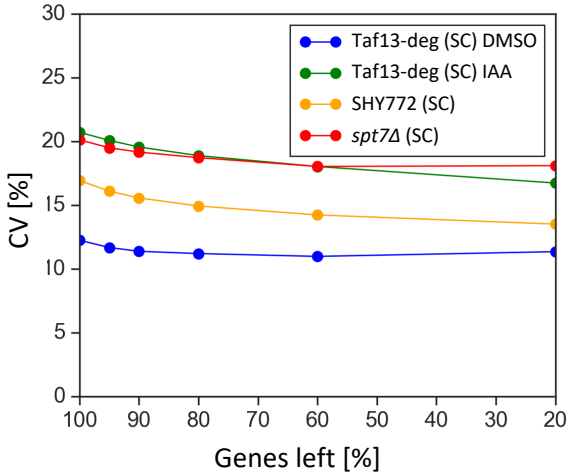
Taf13-deg (SC) DMSO
Taf13-deg (SC) IAA
SHY772 (SC)
spt7Δ (SC)
CV [%]
Genes left [%]
30
25
20
15
10
5
0
100
90
80
70
60
50
40
30
20

B

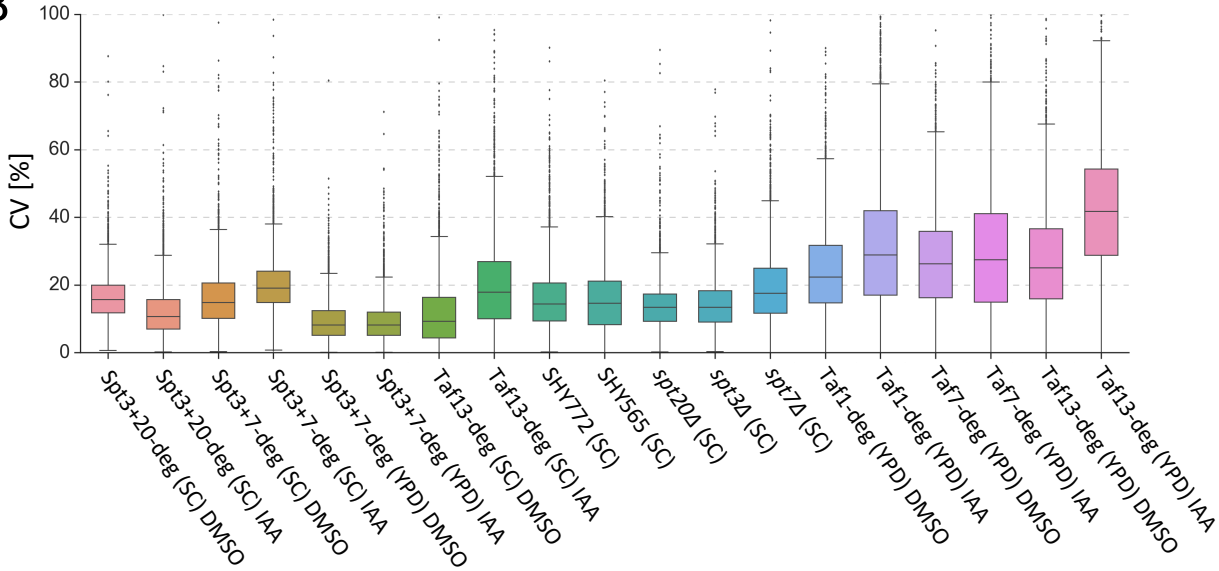
CV [%]
100
80
60
40
20
0
Spt3+20-deg (SC) DMSO
Spt3+20-deg (SC) IAA
Spt3+7-deg (SC) DMSO
Spt3+7-deg (SC) IAA
Spt3+7-deg (YPD) DMSO
Spt3+7-deg (YPD) IAA
Taf13-deg (SC) DMSO
Taf13-deg (SC) IAA
SHY772 (SC)
SHY565 (SC)
spt20Δ (SC)
spt3Δ (SC)
spt7Δ (SC)
Taf1-deg (YPD) DMSO
Taf1-deg (YPD) IAA
Taf7-deg (YPD) DMSO
Taf7-deg (YPD) IAA
Taf13-deg (YPD) DMSO
Taf13-deg (YPD) IAA

C

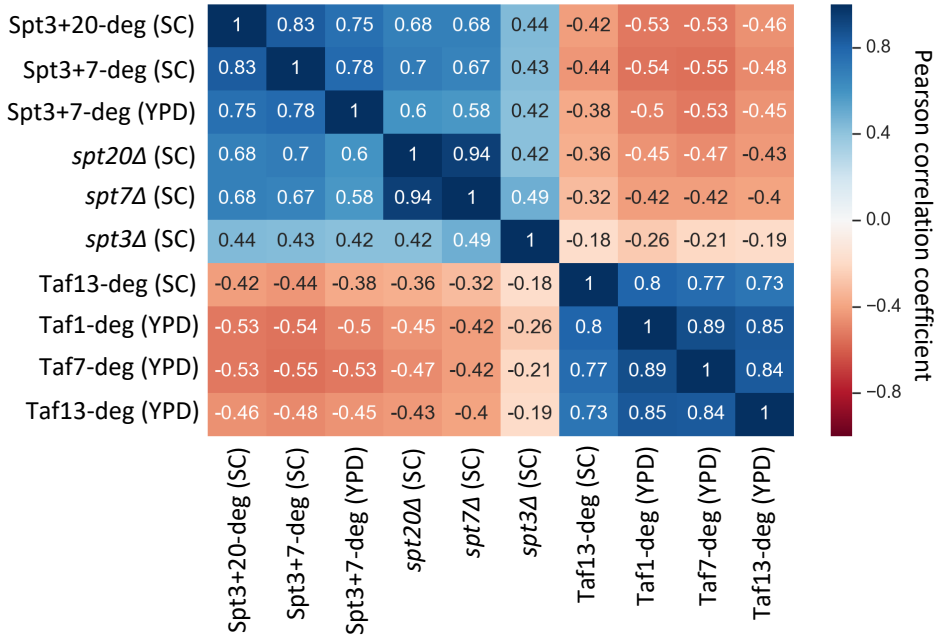
Spt3+20-deg (SC) 1 0.83 0.75 0.68 0.68 0.44 -0.42 -0.53 -0.53 -0.46
Spt3+7-deg (SC) 0.83 1 0.78 0.7 0.67 0.43 -0.44 -0.54 -0.55 -0.48
Spt3+7-deg (YPD) 0.75 0.78 1 0.6 0.58 0.42 -0.38 -0.5 -0.53 -0.45
spt20Δ (SC) 0.68 0.7 0.6 1 0.94 0.42 -0.36 -0.45 -0.47 -0.43
spt7Δ (SC) 0.68 0.67 0.58 0.94 1 0.49 -0.32 -0.42 -0.42 -0.4
spt3Δ (SC) 0.44 0.43 0.42 0.42 0.49 1 -0.18 -0.26 -0.21 -0.19
Taf13-deg (SC) -0.42 -0.44 -0.38 -0.36 -0.32 -0.18 1 0.8 0.77 0.73
Taf1-deg (YPD) -0.53 -0.54 -0.5 -0.45 -0.42 -0.26 0.8 1 0.89 0.85
Taf7-deg (YPD) -0.53 -0.55 -0.53 -0.47 -0.42 -0.21 0.77 0.89 1 0.84
Taf13-deg (YPD) -0.46 -0.48 -0.45 -0.43 -0.4 -0.19 0.73 0.85 0.84 1
Spt3+20-deg (SC)
Spt3+7-deg (SC)
Spt3+7-deg (YPD)
spt20Δ (SC)
spt7Δ (SC)
spt3Δ (SC)
Taf13-deg (SC)
Taf1-deg (YPD)
Taf7-deg (YPD)
Taf13-deg (YPD)
0.8
0.4
0.0
−0.4
−0.8
Pearson correlation coefficient

A

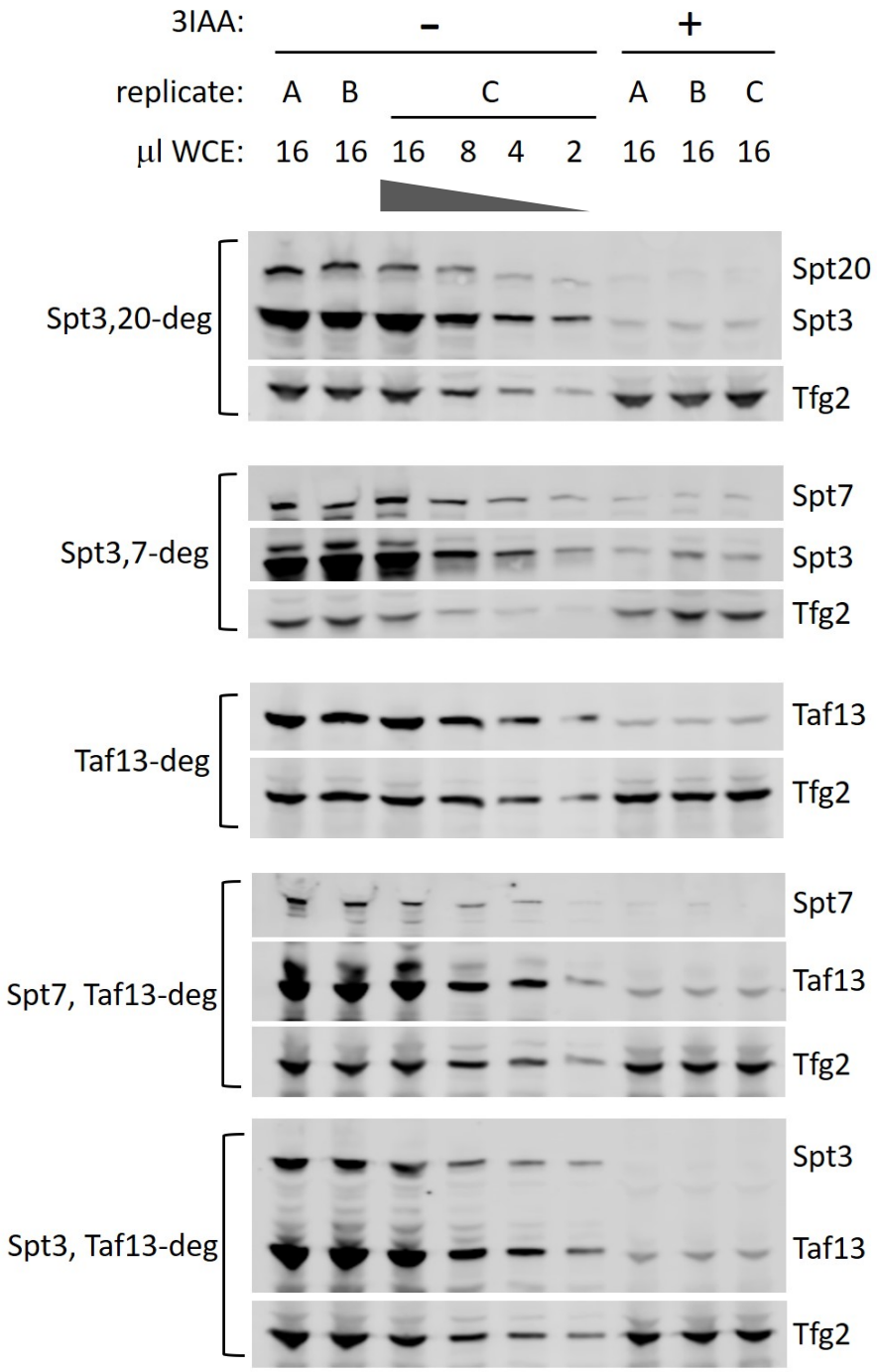
3IAA:
-
+
replicate:
A
B
C
A
B
C
µl WCE:
16
16
16
8
4
2
16
16
16
Spt3,20-deg
Spt20
Spt3
Tfg2
Spt3,7-deg
Spt7
Spt3
Tfg2
Taf13-deg
Taf13
Tfg2
Spt7, Taf13-deg
Spt7
Taf13
Tfg2
Spt3, Taf13-deg
Spt3
Taf13
Tfg2

B

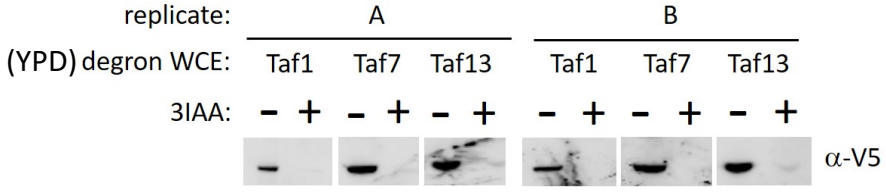
replicate:
A
B
(YPD) degron WCE:
Taf1
Taf7
Taf13
Taf1
Taf7
Taf13
3IAA:
- + - + - +
- + - + - +
α-V5

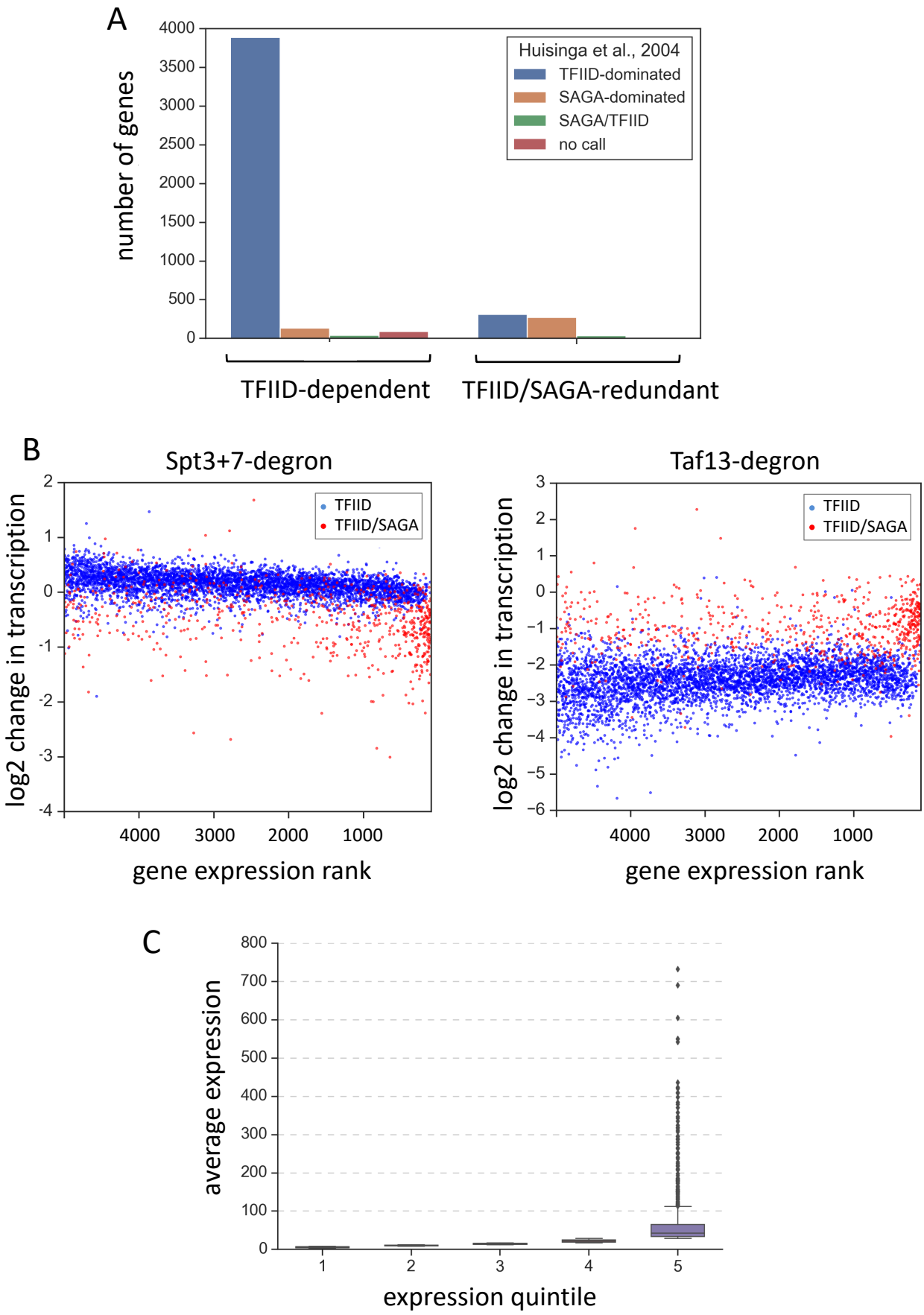
A
number of genes
4000
3500
3000
2500
2000
1500
1000
500
0
Huisinga et al., 2004
TFIID-dominated
SAGA-dominated
SAGA/TFIID
no call
TFIID-dependent
TFIID/SAGA-redundant
B
Spt3+7-degron
log2 change in transcription
TFIID
TFIID/SAGA
gene expression rank
Taf13-degron
log2 change in transcription
TFIID
TFIID/SAGA
gene expression rank
C
average expression
expression quintile

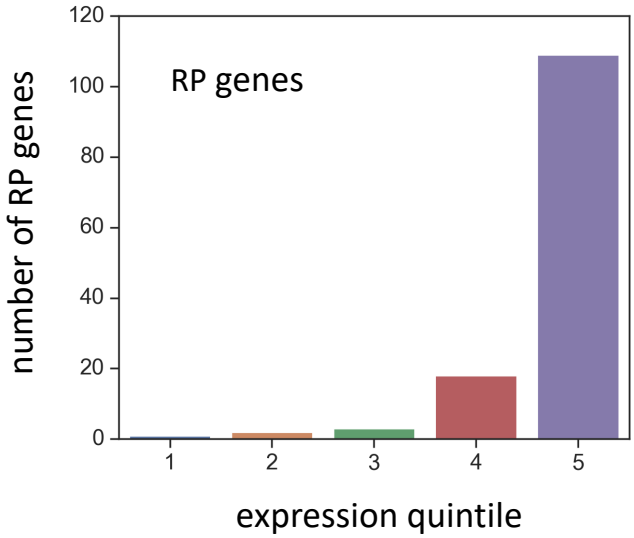
RP genes
number of RP genes
120
100
80
60
40
20
0
1
2
3
4
5
expression quintile

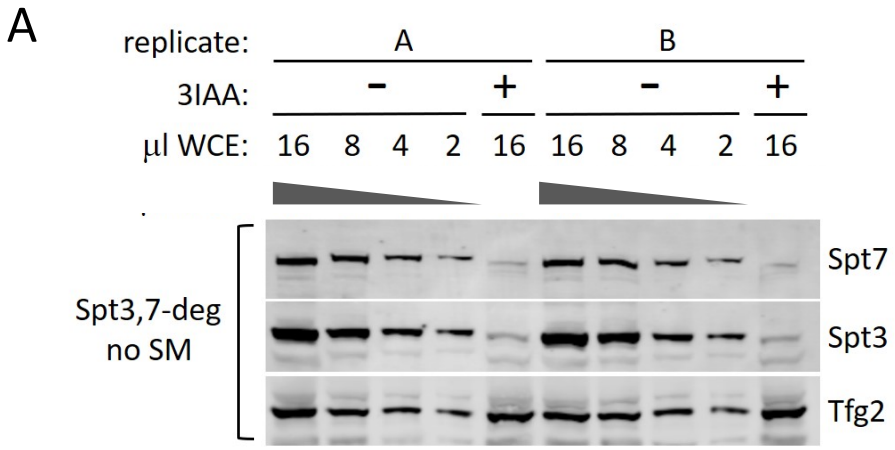
A
replicate:
A
B
3IAA:
-
+
-
+
µl WCE:
16 8 4 2 16 16 8 4 2 16
Spt3,7-deg
no SM
Spt7
Spt3
Tfg2

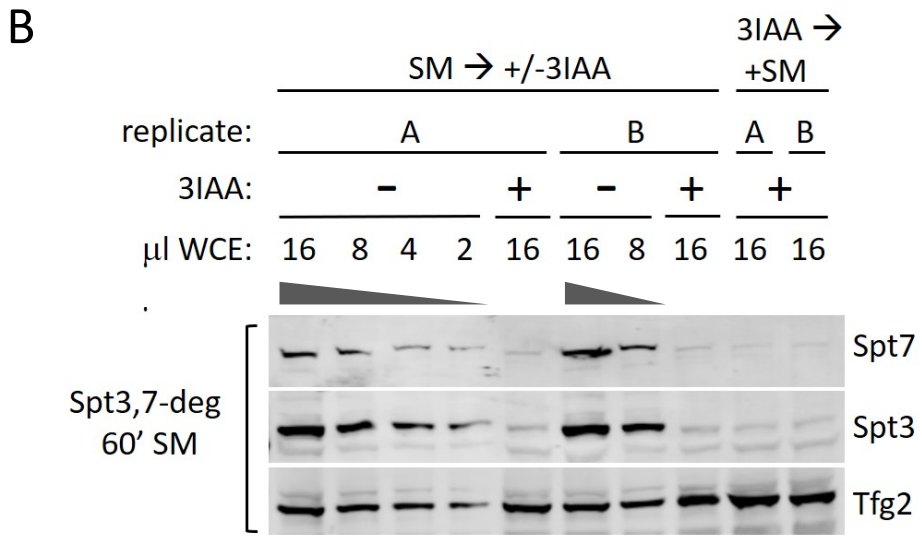
B
SM → +/-3IAA
3IAA →
+SM
replicate:
A
B
A
B
3IAA:
-
+
-
+
+
µl WCE:
16 8 4 2 16 16 8 16 16 16
Spt3,7-deg
60' SM
Spt7
Spt3
Tfg2